

Organization/ Organization Linnéuniversitetet Institution för Teknik Avdelning för Byggteknik		Författare/ Author(s) Firas Salman, Mouhammed Hussain
Linnaeus University School of Engineering Department of Civil Engineering		
Dokumenttyp/Type of document Examensarbete/Degree project	Handledare/tutor Hamid Movaffaghi	Examinator/examiner Hamid Movaffaghi
Titel och undertitel/Title and subtitle		
Jordbävningssäkra Trähus / Earthquake Resistant Wooden House		
Sammanfattning (på svenska)		
<p>Skjuvväggar av trä används ofta för att ge stabilitet åt horisontalbelastade träshustommar. Därför är kunskaper om skjuvväggars deformationsegenskaper nödvändiga för att kunna förbättra utformningen av trästommar utsatta för jordbävningsslaster. Syftet med detta examensarbete är att visa på olika sätt som ökar skjuvväggars absorberande energi eller dämpningskapacitet och som därigenom ger möjligheter att förbättra trästommars motstånd mot jordbävningsslaster.</p> <p>Utgångspunkten har varit laboratorieexperimenten avseende spikförbandens deformationsegenskaper. Syftet med experimenten var att bestämma materialegenskaper för två olika spikförband. Materialsambanden användes därefter som indata i finita element (FE) modeller av skjuvväggselement utsatta för växlande sidobelastning. FE resultaten har visat att skjuvväggars totala dämpningskapacitet beror i huvudsak på spikförbandets materialegenskaper, antal spikförband, väggdimensionen och användningen av mellanreglar.</p>		
Nyckelord Skjuvväggar, Jordbävningsslaster, Dämpningskapacitet, Material indata, FE modell, Spikförband.		
Abstract (in English)		
<p>Wood-stud shear walls are commonly used to provide lateral stability against horizontal forces in wood houses. Therefore, accurate predictions of the deformation properties of shear walls are necessary in order to improve the design of wood frame houses against earthquake loading. The aim of this thesis is to increase damping capacity of wood-stud shear walls and hence improve wood frame houses resistance against earthquake.</p> <p>The starting point has been the laboratory experiments of nail joint's deformation properties. Purpose of the experiments was to determine material properties of a nail joint. The material properties have later been used as material input data in the finite element (FE) model of wood-stud shear wall elements under alternating lateral loading. FE results have shown that wood-stud shear wall element's damping capacity is mainly dependent on nail joints properties, number of nail joints, wall dimension and the use of middle studs.</p>		
Key Words Shear walls, Earthquake loading, Damping capacity, Material data, FE model, Nail joint.		
Utgivningsår/Year of issue 2010	Språk/Language English	Antal sidor/Number of pages 50
Internet: www.lnu.se		

Abstract

Wood-stud shear walls are commonly used to provide lateral stability against horizontal forces in wood houses. Therefore, accurate predictions of the deformation properties of shear walls are necessary in order to improve the design of wood frame houses against earthquake loading. The aim of this thesis is to increase damping capacity of wood-stud shear walls and hence improve wood frame houses' resistance against earthquakes.

The starting point has been the laboratory experiments of nail joint's deformation properties. Purpose of the experiments was to determine material properties of a nail joint. The material properties have later been used as material input data in the finite element (FE) model of wood-stud shear wall elements under alternating lateral loading. FE results have shown that wood-stud shear wall element's damping capacity is mainly dependent on nail joints properties, number of nail joints, wall dimension and the use of middle studs.

Key Words: Shear walls, Earthquake loading, Damping capacity, Material data, FE model, Nail joint

Acknowledgement

This thesis was performed during the spring of 2010 at the department of Civil Engineering at Linnaeus University.

We would like to extremely thank our supervisor Doctor Hamid Movaffaghi for his great assistance and support. He was so helpful and patient during all the steps of our thesis work from the beginning to the end. He did not ever hesitate to give any support and to advise us about each individual issue concerning our thesis. His technical background about the shear wall and his professional knowledge on the computer software Abaqus/Cae, which we have used for finite element simulations, has made everything clear and easy for us to understand. We are really appreciating his encouragements during the whole project.

Concerning our laboratory works, we would also like to thank Mr. Bertil Enquist and Mr. Jonaz Nilsson for their assistance and cooperation. They have supported our laboratory works, where all the test specimens for load-deformation-relationship measurements have constructed and conducted. Mr. Bertil has saved no effort to explain and learn us about every thing concerning the machines and instruments that we have used. Mr. Jonaz Nilsson has helped us with cutting the wood material for all specimens. We are so thankful for all their support.

Växjö/Sweden
May 2010

Table of contents

<i>Abstract</i>	<i>III</i>
<i>Acknowledgement</i>	<i>IV</i>
<i>Table of contents</i>	<i>V</i>
1. Introduction	1
1.1 Background	1
1.2 Purpose and aim	3
1.3 Hypothesis and limitations	4
2. Literature review	5
3. Theory	6
4. Method	6
4.1 Laboratory experiments	7
4.2 FE model of nail joint	13
4.3 FE model of shear wall element	14
5. FE results	18
5.1 FE- results verification	19
6. Analysis of FE results	20
6.1 Top displacemen of shear wallt	20
6.2 Damping capacity of the shear wall element	21
6.3 Effect of different configurations on damping capacity	21
6.3.1 Effect of nail joint distribution	22
6.3.2 Influence of the panel's width	23
6.3.3 Influence of middle studs	25
6.4 Relationship between prescribed and relative displacements of nail joint	26
7. Discussions and Conclusions	28
8. References	29
9. Appendix	31

1. Introduction

1.1 Background

Wood is considered as one of the most important and reliable construction materials, since it is a renewable and has high resistance to earthquakes due to its properties. It has been used as a building material for thousands of years ago and still in the stage of research and development. One of the important research areas is enhancing earthquake resistance of the wooden frame house in the earthquakes prone regions.

There were about 15000 earthquakes happened in different parts of the world year 2009, most of these earthquakes cause no damages [18].

Figure 1 below shows the structural damage of wood frame houses from Niigata in Japan [14].



Figure 1. Damaged wood frame houses from Niigata prefecture in Japan, Oct. 2004, magnitude 6.8 on Richter scale [14].

Wooden frames behave well in case of earthquakes because of, among other things, their low weight and high degree of static indeterminacy. This has been verified through the history.

Wood-stud shear wall is normally used as a stabilizing element when the frame is subjected to alternating lateral loads in its plane. Shear walls are normally consisting of wood-stud frame and boards. The boards are usually nailed to wood-stud with small c/c spacing to achieve sufficient stiffness and strength [3].

The response of wooden frames as they subjected to dynamic loads, such as wind and earthquakes, is mainly determined by shear wall's damping properties, which in turn depends on the nail joint's hysteresis energy absorption or damping capacity. This means that the plastic deformation occurs in the nail joints while both the boards and studs are elastic and stiff [3].

Figure 2 below shows two major functions of a shear wall, i.e. stiffness to control the drift and strength to resist shear forces [2].

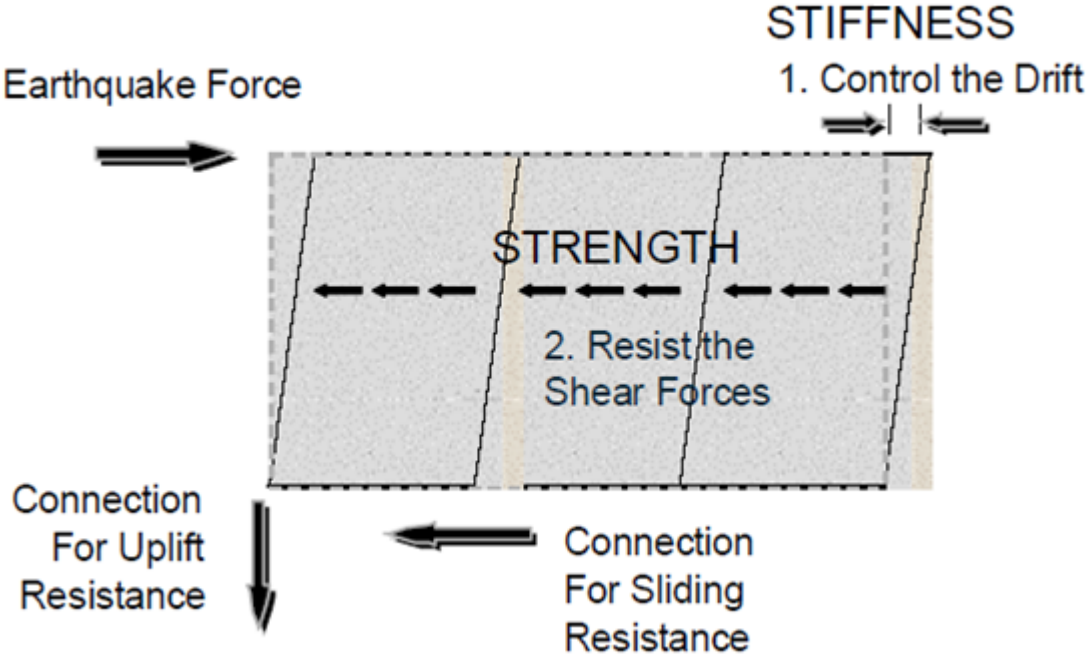


Figure 2. Two Major functions of a shear wall: control the drift and resist the shear forces.

A general problem for all timber-based structures is the failure due to fatigue. As a result, fatigue failure reduces the serviceability time of the wooden structures, because of the damages arising due to the cyclic load [12].

1.2 Purpose and aim

The aim of the thesis is to increase the damping capacity of wood-stud shear walls in order to strengthen earthquake resistance of wooden houses. Design improvement can be done, among others, by enhancing shear walls' design and appropriately positioning such a wall in the plan of wood frame.

The starting point has been the laboratory experiments of nail joint's deformation properties. Purpose of the experiments was to determine material properties of a nail joint. The material properties have later been used as a material input data in the finite element (FE) model of wood-stud shear wall elements under alternating lateral loading.

Figure 3 below shows a typical shear wall and its associated shear wall element (1.2 x 2.4) m².

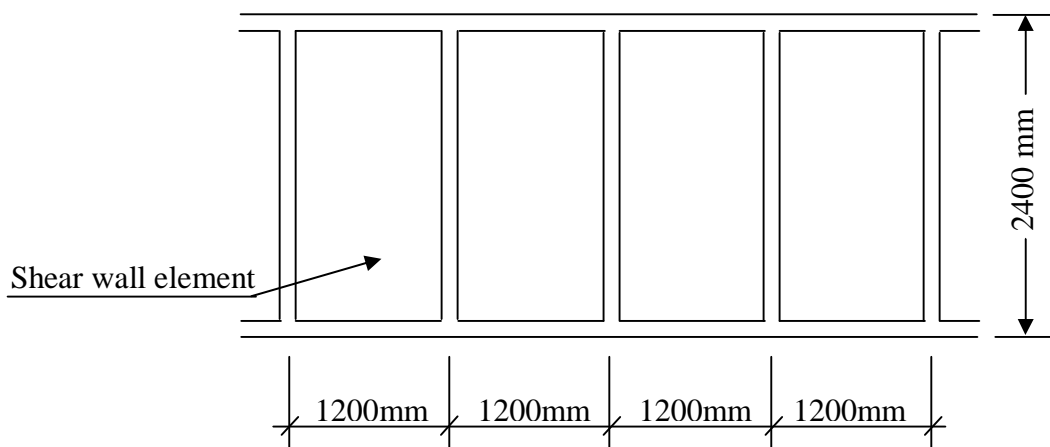


Figure 3. A Typical Shear wall and its associated shear wall elements.

Figure 4 below shows the studied wood-stud shear wall element. It has been assembled by two plywood panels that have been nailed to a wood-stud frame.

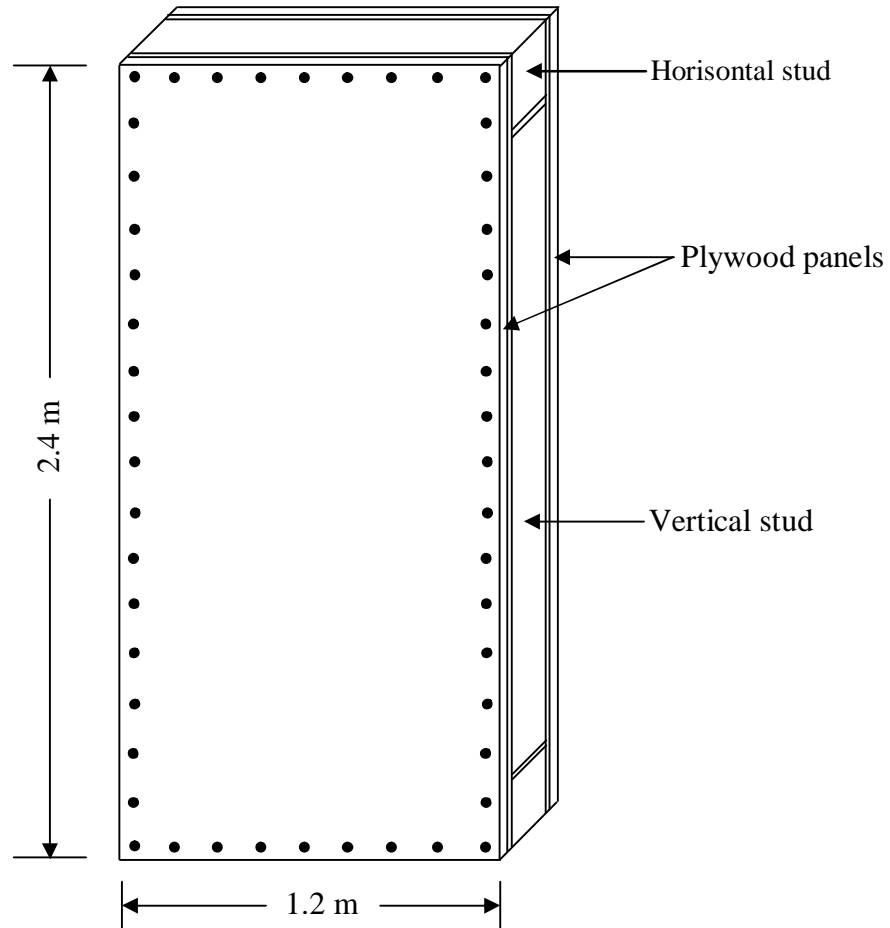


Figure 4. The studied shear wall element and its components.

1.3 Hypothesis and limitations

The focus has been on improving shear wall elements' design against earthquake loading. FE analyses have been performed for a limited number of shear wall element models with different geometrical configurations. The restrictions and simplifications being made are summarized as follows:

- ❖ A real dynamic load from the earthquake is replaced with a horizontal, alternating, static load at top left corner of the shear wall element.
- ❖ Friction forces affecting the hysterical curves in both experiment and FE model are included in the elastic-plastic material parameters for nail joint.
- ❖ Nail's type and the corresponding c/c spacing are according to Appendix A1.
- ❖ Boarding material for shear wall element is made of the plywood with properties according to section 4.3.
- ❖ Wood-stud frame with dimension $(1.2 \times 2.4) \text{ m}^2$ without middle studs is chosen as the standard shear wall element.
- ❖ Influence of openings such as windows, doors, etc. on shear wall element will not be considered.
- ❖ Deformations out of plane of the shear wall element are neglected.

2. Literature review

One important issue, concerning shear wall, is the position of such a wall. They should always be placed in such a way that a symmetrically distributed stiffness occurs. This reduces the tendency of twisting deformation around vertical axis. The Figure 5 below shows example of a symmetrically distributed shear walls inside the building [1].

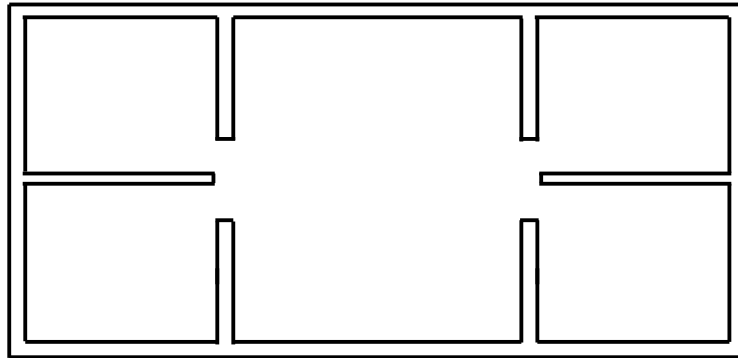


Figure 5. A possible symmetrical placement of shear walls inside the building.

Figure 6 below shows a **deformed** and **undeformed** shear wall element. When a shear wall element is loaded in its plane, the following happens: nails will deform, wood-stud frame will deform as a parallelogram, while the panels keep their rectangular shape. Corners' nails deformation direction is parallel to the shear wall element diagonals [4].

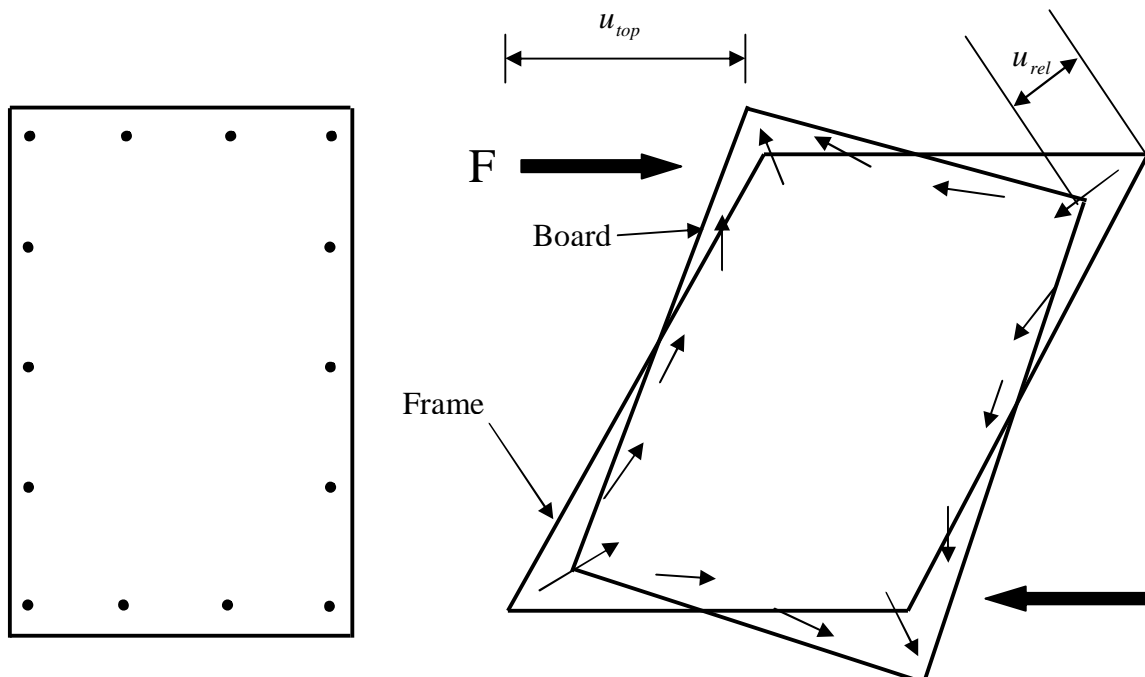


Figure 6. A deformed and undeformed shear wall element under transversal loading.

If the wood material is very stiff, the energy will mainly be absorbed by the nail joints. Nail's type and joint's design should be chosen with respect to the permitted deflection (u_{top}) for shear wall element [1].

We have studied the relationship between the top displacement u_{top} and the relative displacement u_r in section 6.4.

3. Theory

We have used Abaqus/Cae for both modeling and simulation. Abaqus/Cae is a general purpose computer program based on finite element (FE) method. Its special strength is the non-linear simulations. The FE method is a numerical method to solve the differential equation systems. It has been developed mainly to solve engineering problems.

The FE method restates the differential equations into integral equations, by inserting an approximate solution into integral equations. Unknown coefficients at nodes can be calculated by solving a system of ordinary differential equations of equilibrium as:

$$K\tilde{u} = F$$

Where K , \tilde{u} and F are respectively, stiffness matrix of the structure, unknown nodal displacements and the external load vector [12].

Problems with non-linear stress-strain relations will yield a system of nonlinear equations according to:

$$F_{\sigma}\tilde{u} = F$$

Where F_{σ} is the non-linear internal force [12].

4. Methods

The starting point has been the laboratory experiments concerning nail joint's non-linear deformation properties. The purpose of experiments was to measure the force-deformation relationship and with help of these measurements determine the stress-strain relationship of the nail joint. The material model of nail joint has later been used in the FE model of wood-stud shear wall elements under alternating lateral loading.

The shear wall element that we have studied consists of two plywood boards that are nailed to a wood-stud frame. Its geometry and dimensions are shown in the Figure 7.

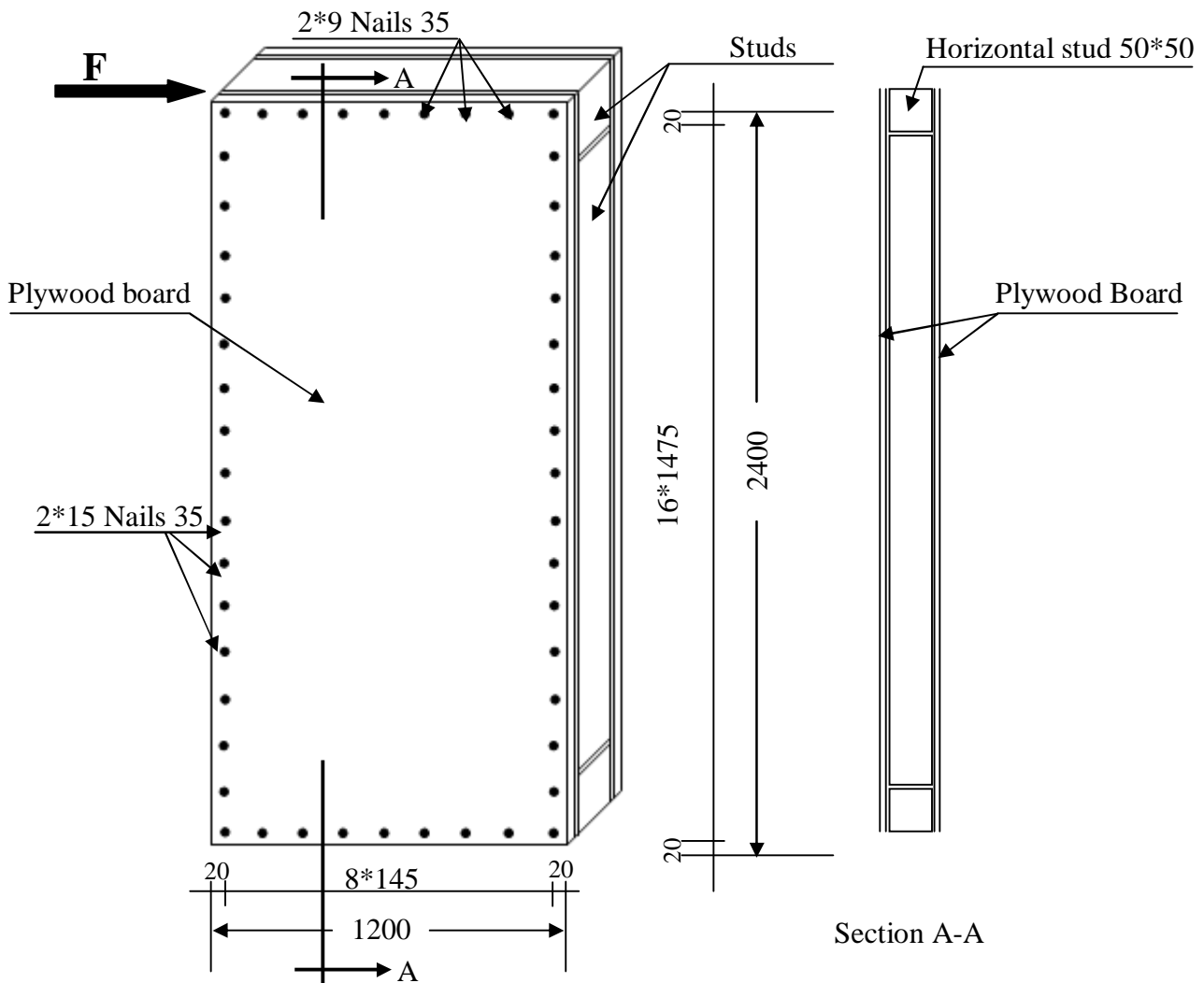


Figure 7. A shear wall element's geometry and dimensions (all dimensions are in mm).

4.1 Laboratory experiments

The purpose of the laboratory experiments was to determine stress-strain relationship for a nail joint. The material model has later been used for the beam elements that represent the nail joint in the FE model of a shear wall element. See section 4.3.

Test specimens were built up of 12 mm thick sheets of plywood, P30, nailed with 35 x 1.7 x 1.7 mm³ nails on both sides of a 50 x 50 x 300 mm³ wooden stud, see Figure 8 below. On the right side of the Figure 8, 2 x 4 nails were nailed to the wood. These nails have been tested and evaluated. On the left side, wood and plywood were assembled by using both several nails and adhesive bonding.

The deformation measurement points are the points where the movement between points 1 and 2 are going to be measured according to the Figure 8.

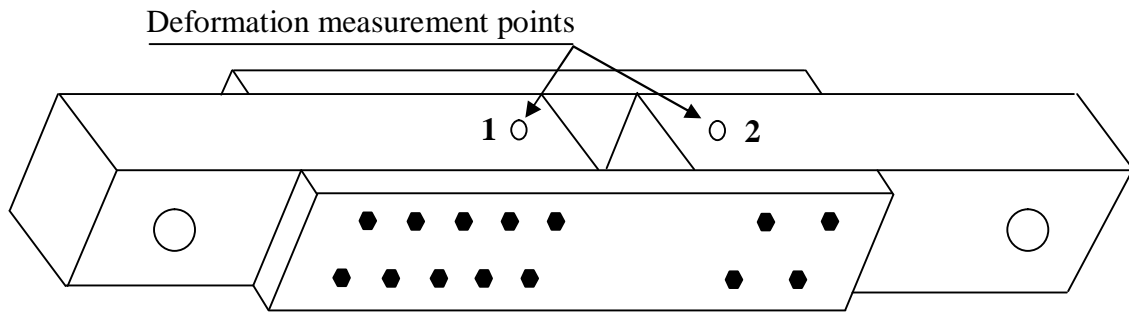


Figure 8. Design of test specimen and the deformation measurement points.

Test specimens were loaded with a uni-axial alternating tensile and compressive force. A prescribed alternating displacement amplitude of $\pm 2 \text{ mm}$ was used for the nail joint in the experiment. The 2 mm amplitude has judged to be very close to the fatigue failure limit of a nail joint during an earthquake that maybe will last in less then 30 seconds [1].

Totally 16 specimens were loaded according to Table 1. The alternating loading was carried out for three cycles. Half of the specimens were nailed using 1.7 mm diameter nails and the rest with 2 mm diameter nails. Load was applied in displacement control with a speed of 0.1 mm/s. This displacement rate is so low that the load can be regarded as static.

Specimen	Load to grain direction	Failure load (kN)	Constant displacement	Nail diam. (mm)	Board's type	Remarks
A-01	0	-	+/-2 mm	1.7	Plywood	With Glue
A-02	0	-	+/-2 mm	1.7	Plywood	
A-03	0	-	+/-2 mm	1.7	Plywood	
A-04	0	2.84	-	1.7	Plywood	
B-01	0	-	+/-2 mm	1.7	OSB	With Glue
B-02	0	-	+/-2 mm	1.7	OSB	
B-03	0	-	+/-2 mm	1.7	OSB	
B-04	0	2.86	-	1.7	OSB	
C-01	0	-	+/-2 mm	2.0	Plywood	With Glue
C-02	0	-	+/-2 mm	2.0	Plywood	
C-03	0	-	+/-2 mm	2.0	Plywood	
C-04	0	4.04	-	2.0	Plywood	
D-01	0	-	+/-2 mm	2.0	OSB	With Glue
D-02	0	-	+/-2 mm	2.0	OSB	
D-03	0	-	+/-2 mm	2.0	OSB	
D-04	0	4.83	-	2.0	OSB	

Table 1. Test specimens and the loading.

Material testing machine was of type MTS810 with load capacity of ± 100 kN. Two displacement sensors of type LVDT with measuring capacity of 10 mm were mounted on both sides of the test specimen. With these sensors, the distance between the two points 1 and 2 could be measured during the entire loading. The force, displacement sensors and testing machine are shown in Figure 9.

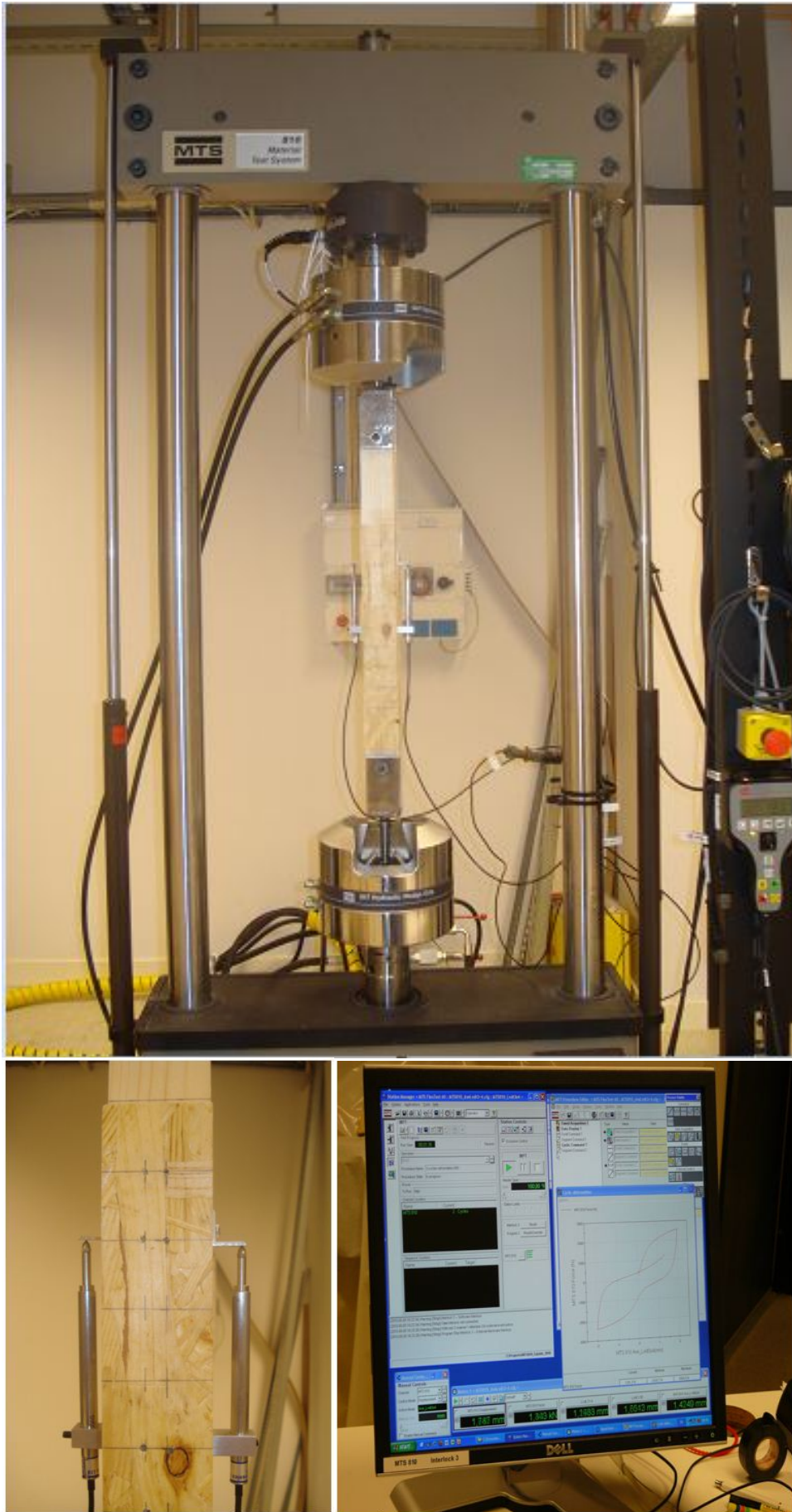


Figure 9. The pictures show the test set-up with the testing machine, measuring equipment with load cell and LVDT: s and test specimen for hysteresis tests according to Table 1.

Figure 10 shows hysteresis loops (3 loops) for test specimen A-01. This test specimen was chosen for further analysis where specimens A-01 to B-03 had almost identical hysteresis loops.

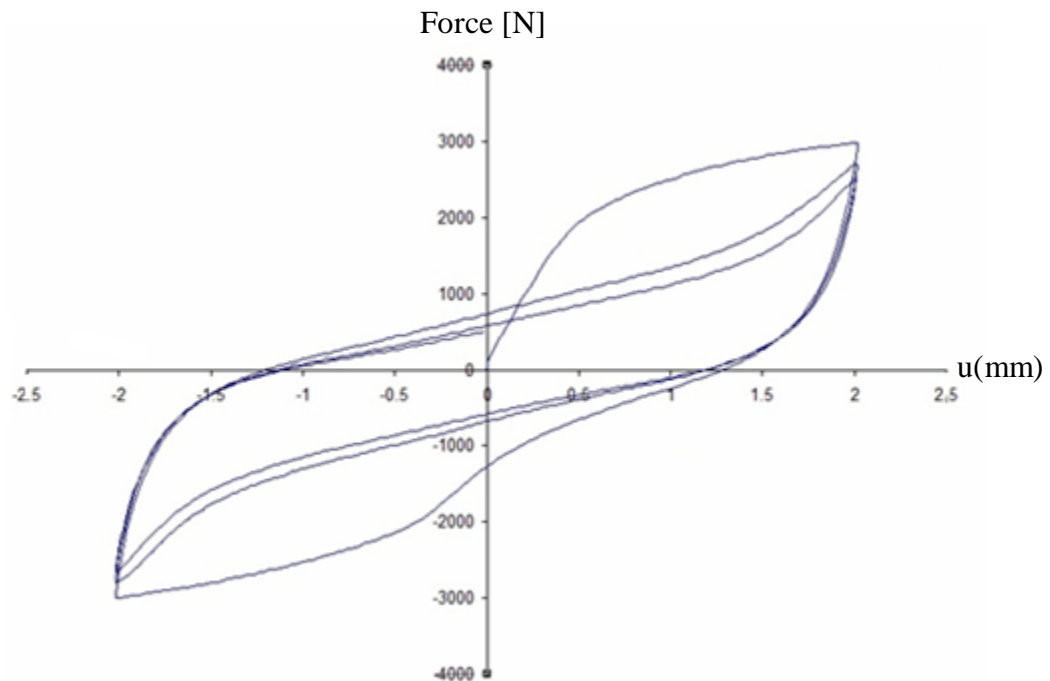


Figure 10. Measured hysteresis (three) loops for test specimen A-01.

Figure 11A shows the extracted force-displacement relation of a single nail joint. The elastic part has been chosen in accordance with the second and third cycle's average slope of the nail-joint in Figure 10 above. All calculations are according to Appendix A2/A3.

The Figure 11B shows the evaluated ideal-plastic material model of the nail-joint extracted from experiment that have been used in FE model of a nail joint in the chapter 4.2. All calculations are according to Appendix A3.

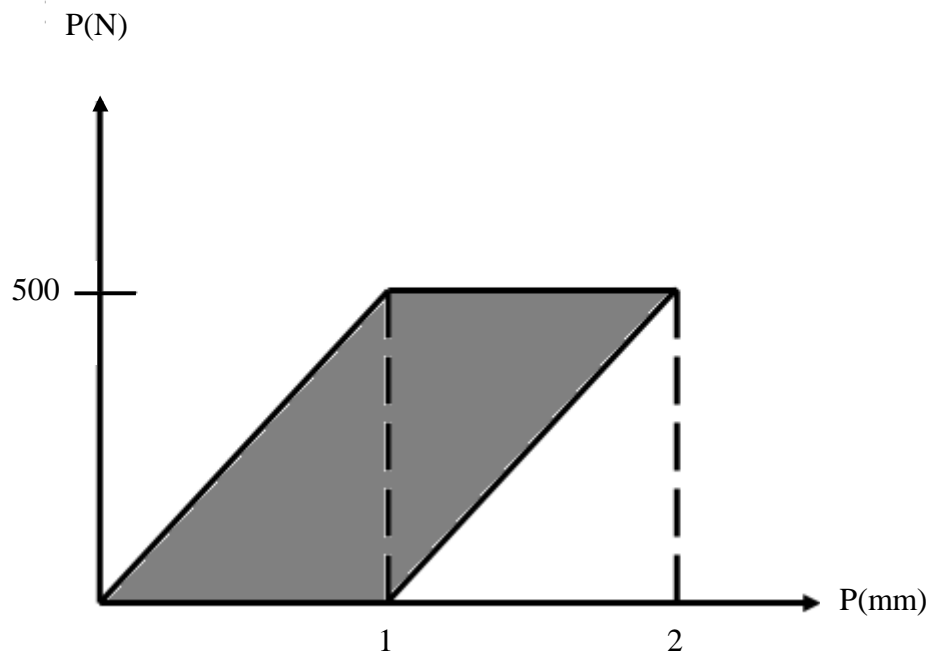


Figure 11A. The extracted force-displacement relation of a single nail joint from experiments.

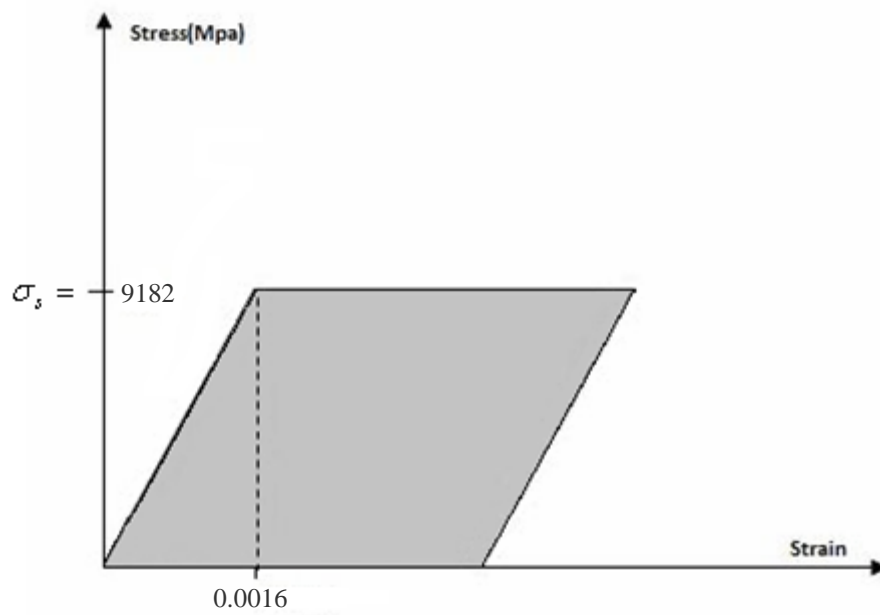


Figure 11B. The extracted ideal-plastic material model a single nail joint from experiments.

4.2 FE model of the nail joint

A nail joint comprises of two nails (one from each side) in the FE model. It has been discretized by a 3-nodes beam element of type B31. Both of the end points of the nail joints are fixed to the panels using MPC constraint. A prescribed displacement of +/- 2 mm has been applied at the middle of the nail joint. The ideal-plastic material model of the nail joint according to the Figure 11B above has been used.

Figure 12 shows both FE model of the single nail joint and displacement contour plot.

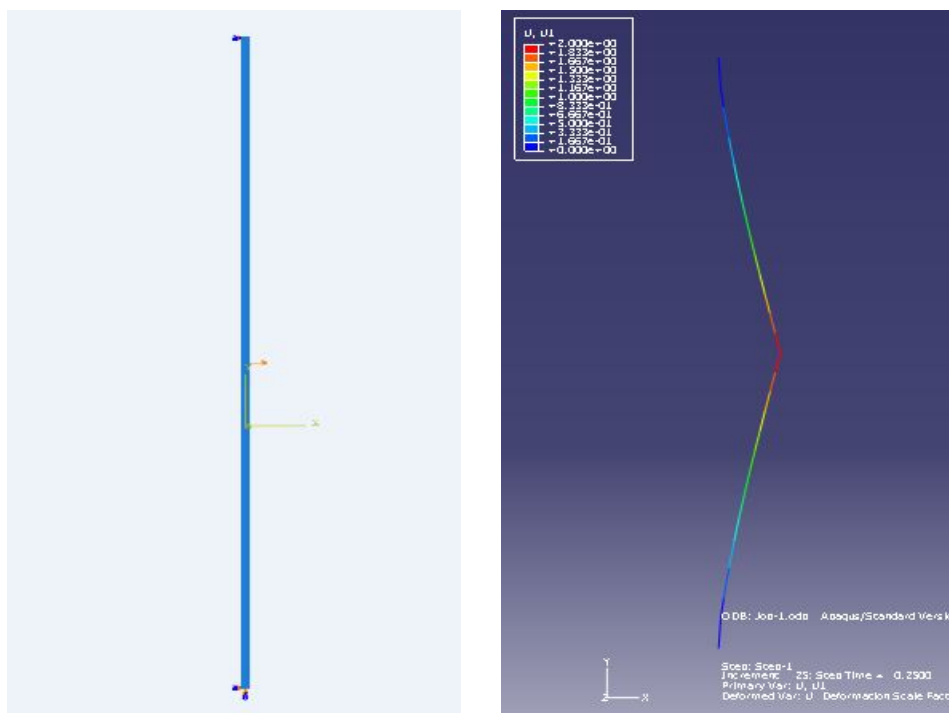


Figure 12. Left: FE model of the single nail joint. Right: Displacement contour plot of the analyzed nail joint.

There were differences in force-displacement relation between FE analysis and the experiment results. In order to calibrate the FE model with the experiment, Young modulus E was changed from $5.88E6 \text{ N/mm}^2$ to $6.25E6 \text{ N/mm}^2$ and the Yield stress σ_s was changed from $9.182E3 \text{ N/mm}^2$ to $8.75E3 \text{ N/mm}^2$.

Figure 13 shows the force-displacement relation for a single nail joint extracted from non-linear FE analysis after calibration. It has good agreement with Figure 10 above. This indicates good calibration of results between FE model of a single nail joint and the experiment.

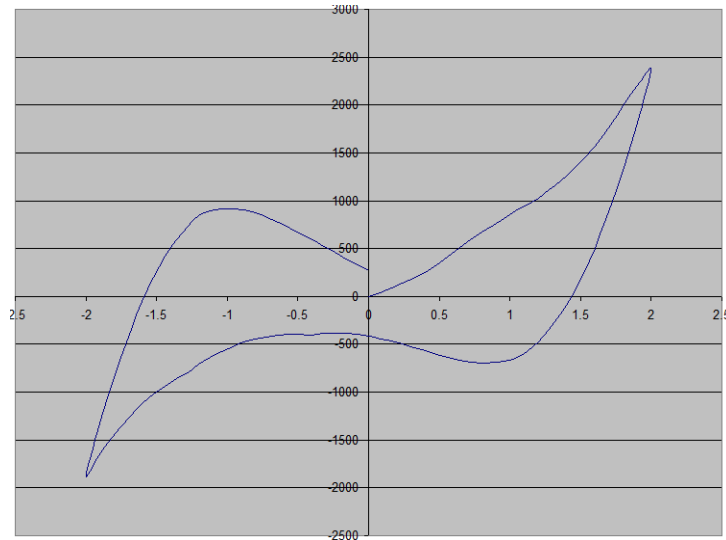


Figure 13. Force-displacement relation for a single nail joint extracted from nonlinear FE analysis.

4.3 FE model of the shear wall element

The shear wall element in Figure 7 above has been analyzed using Abaqus/Cae. Wood and plywood have been modeled with elastic material input data. Nail joint's material properties have been determined from the experiment, see Appendix A2/A3. A horizontal alternating prescribed displacement of ± 9 mm has been applied at left top corner of the frame, see Figure 14 below.

Prescribed displacement ± 9 mm

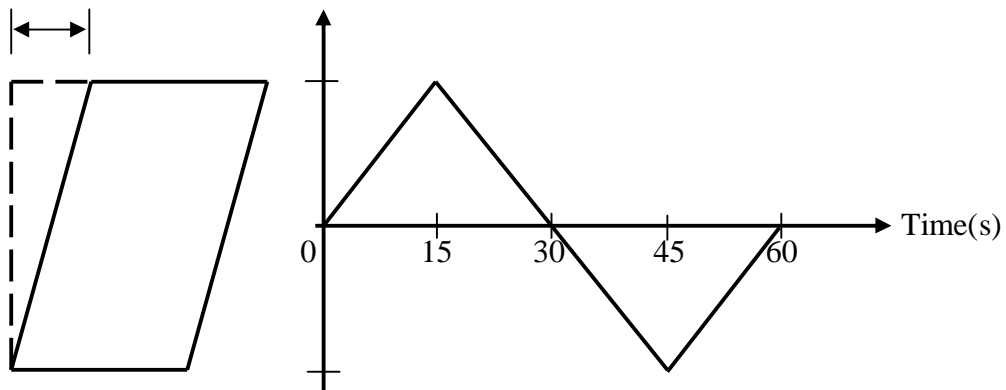


Figure 14. Left: A prescribed alternating displacement ± 9 mm at the top left corner of the shear wall, u_{top} . Right: Prescribed displacement time history in FE analysis.

Several FE models with different geometrical configurations have been analyzed. All the FE models have been fixed to the bottom, see Figure 15.

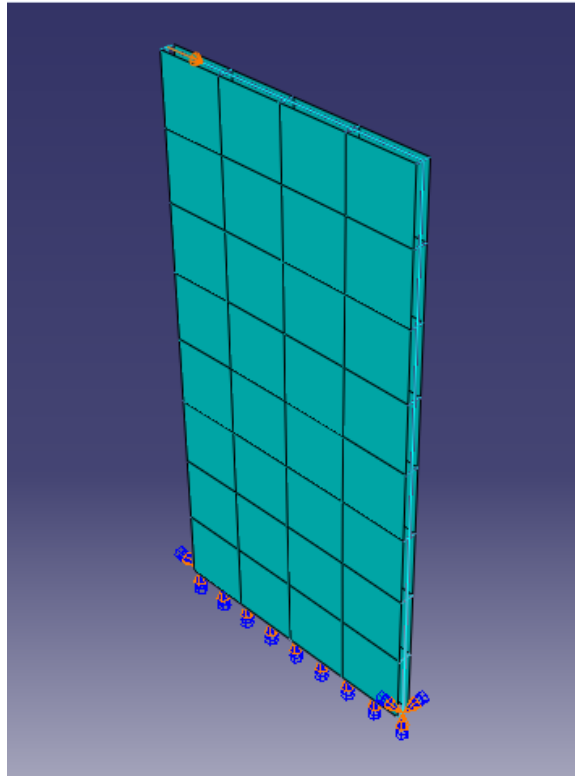


Figure 15. FE model of the standard shear wall element (1.2 x 2.4) m².

Wood-stud has been modeled using 2-nodes beam elements of type B31 with the nodal subdivision according to Figure 16 below. Node subdivisions are compatible with nails c/c-distance. Figure 17 shows the deformed shape of the wood-stud frame. As it mentioned before, the wood-stud frame deforms as a parallelogram.

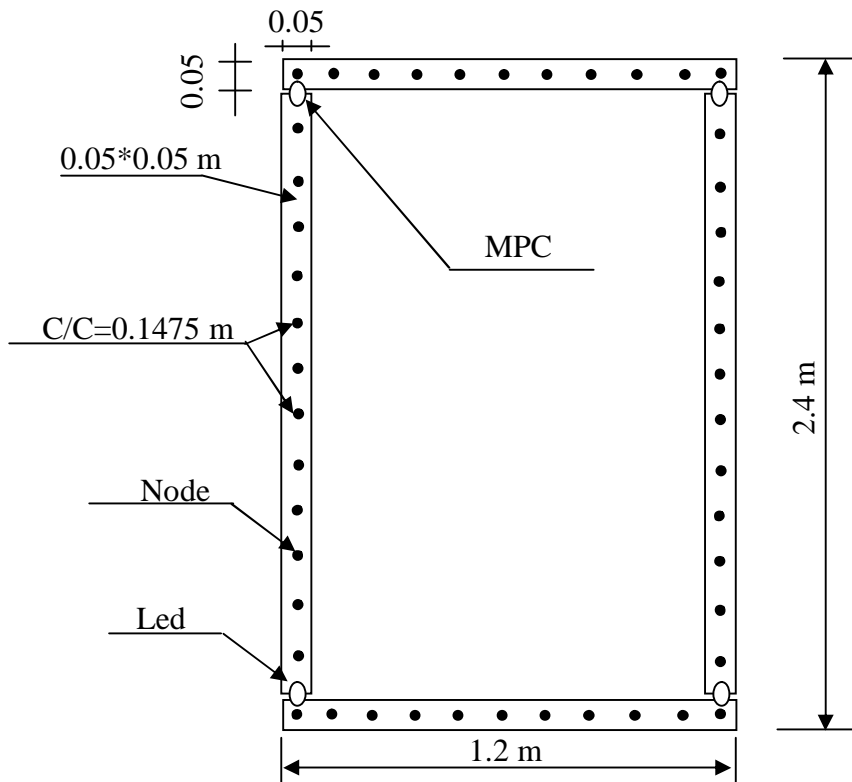


Figure 16. Node subdivisions of wood-stud frame.

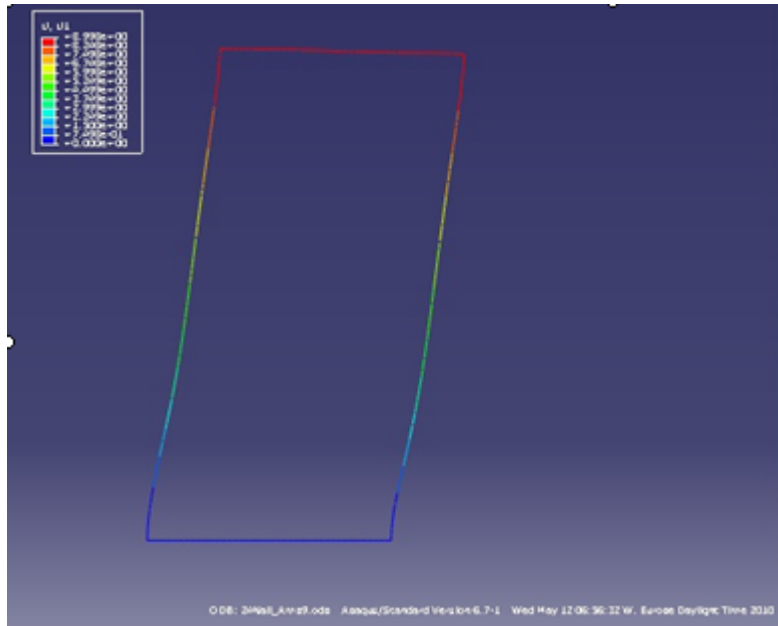


Figure 17. The deformed shape of the wood-stud frame for a standard shear wall element (1.2 x 2.4) m².

Plywood panels with 12 mm thickness have been modeled with 4-nodes shell element type S4R. Node subdivisions are compatible with nails c/c-distance according to Figure 18 below.

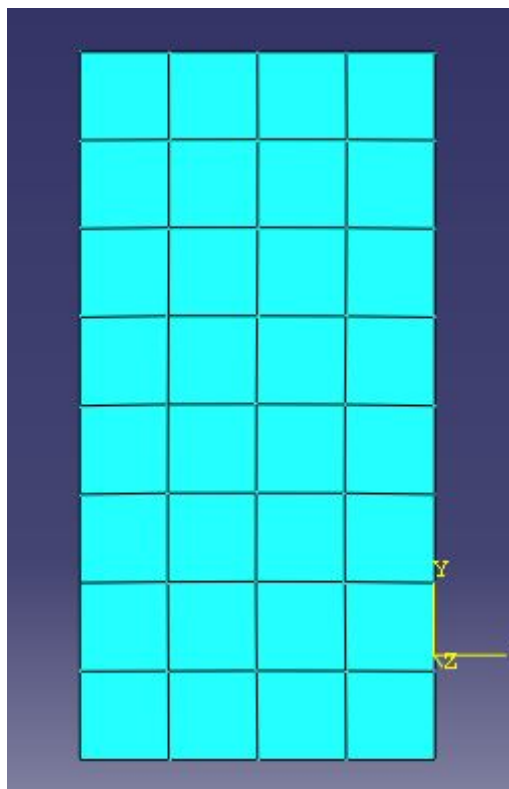


Figure 18. Node subdivisions for the plywood panels.

Nail-joints are discretized with 3-nodes beam element of type B31 with node subdivisions according to Figure 19. Material properties were extracted from Appendix A3.

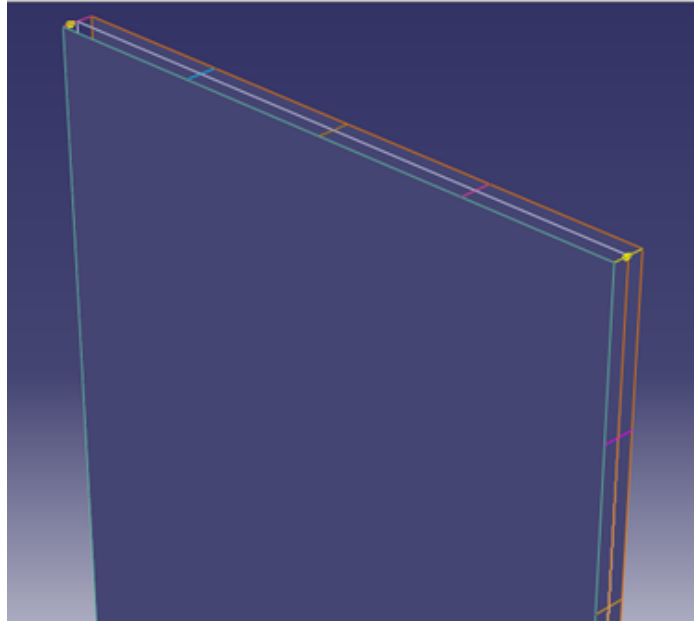


Figure 19. Orientation and position of the beam elements representing the nail-joints.

Material parameters in the FE model are as follows:

1. Plywood panels

Modulus of Elasticity: $E = 6 \times 10^9 \text{ N/m}^2$

Poisson's ratio: $\nu = 0.3$

Thickness: $t = 12 \text{ mm}$

2. Wood-studs

Modulus of Elasticity: $E = 10 \times 10^9 \text{ N/m}^2$

Poisson's ratio: $\nu = 0.3$

Cross-section measurements: $b \times h = 50 \times 50 \text{ [mm}^2\text{]}$

3. Nail joints

Modulus of Elasticity: $E = 6.25 \times 10^6 \text{ N/mm}^2$

Yield stress: $\sigma_s = 8.75 \times 10^3 \text{ N/mm}^2$

Poisson's ratio: $\nu = 0.3$

5. FE results

FE analyses have been performed using Abaqus/Cae version 682 with 1 GB primary memory and 80 GB hard disk. The standard FE model had 1264 elements .CPU time was 15 minutes.

Table 2 below presents the results of FE analysis and the evaluation of total external energy for 8 different computer runs.

Model Name	B x H (m ²)	Number of nail-joints	u_{rel}^{max} [mm]	u_{top} [mm]	F [N]	E [Nmm/cycle]	Notes
W1	0.6 x 2,4	24	0.3	± 9	1025	1000	
W2	1.8 x 2,4	24	2.56	± 9	2955	32160	
W3	1,2 x 2,4	24	1.95	± 9	2616	24000	
W4	1,2 x 2,4	36	1.9	± 9	3520	26000	
W5	1,2 x 2,4	48	1.17	± 9	4600	30000	
W6	1,2 x 2,4	31	1.12	± 9	2795	26800	1 middle stud ⁽¹⁾
W7	1,2 x 2,4	38	1.3	± 9	3400	27600	2 middle studs ⁽¹⁾

Table 2. Summary of FE analysis results

Where;

(1) = Simulation with middle stud/s

B = Board's width

H = Board's height

u_{rel}^{max} = Maximum relative displacement for the nail

u_{top} = Prescribed displacement at the top left corner of shear wall element

F = Wall reaction force

E = Total external damping capacity per cycle

5.1 FE model verification

Both the mesh size and element order of the FE model for the nail joint have been verified. Figure 20 below shows the results in terms of damping capacity for FE model with 4 different mesh sizes for nail joint and second order elements.

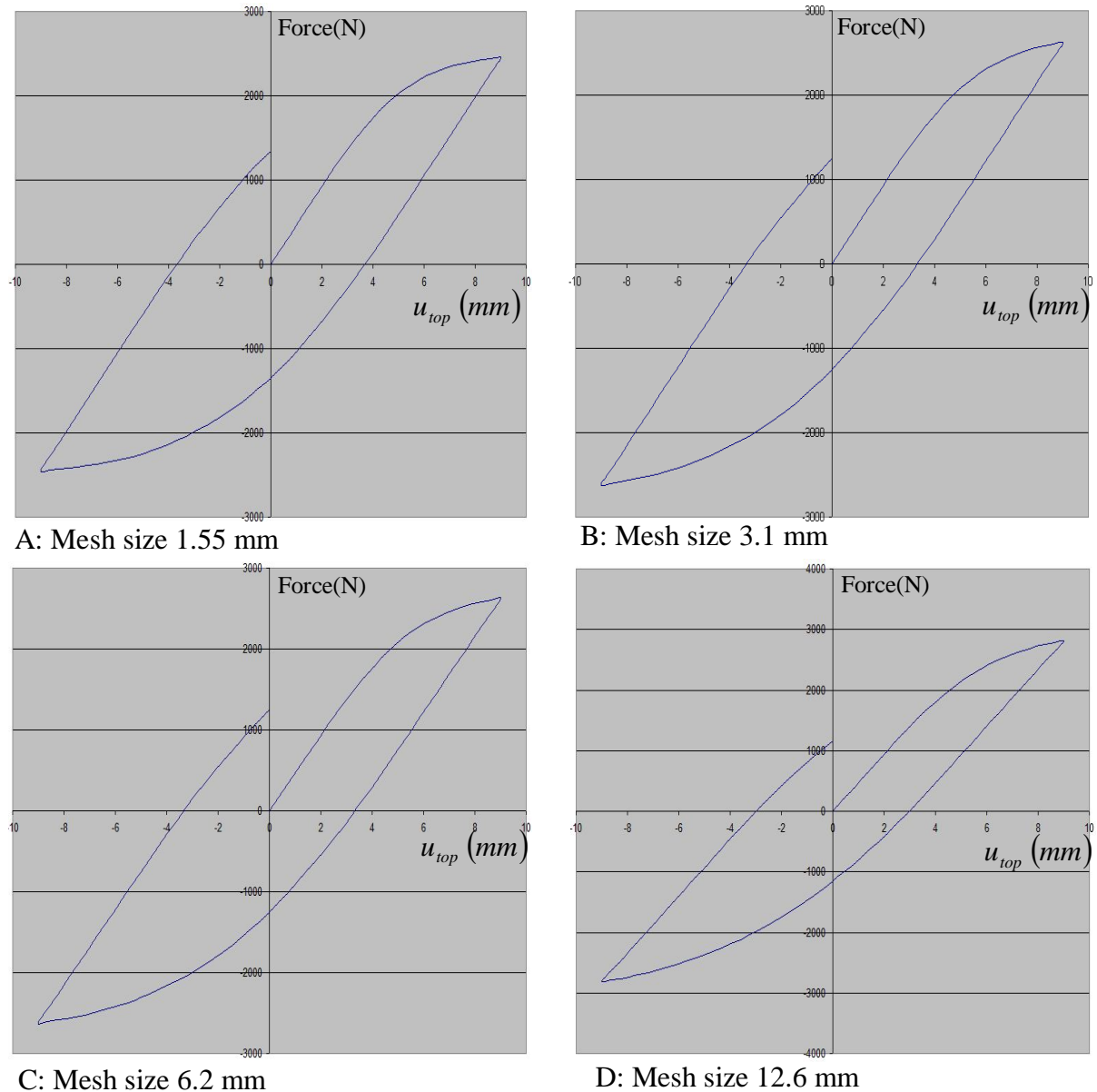


Figure 20. Shear wall element's damping capacities with A: mesh size 1.55 mm B: mesh size 3.1 mm C: mesh size 6.2 mm D: mesh size 12.4 mm.

Differences in damping capacities between the 4 meshes are very small, i.e. less than 2%. Thus FE model with low mesh density judged to be verified with respect to both mesh size and element order.

6. Analysis of FE results

6.1 Top displacement of shear wall element

Figure 21 below shows the relative and top displacements for a deformed shear wall element.

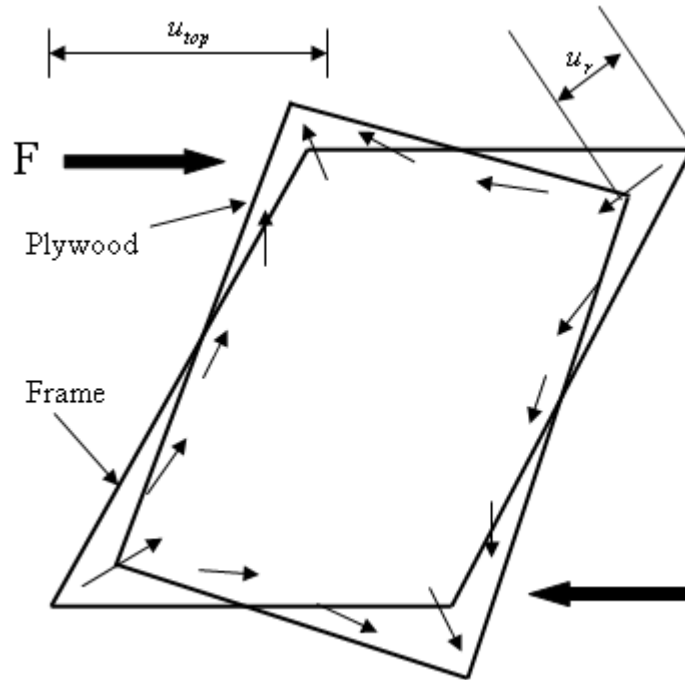


Figure 21. The prescribed displacement and force at the top left corner of the shear wall element.

Top displacement u_{top} of shear wall element should be limited so that highest 25% of the total number of nails gets a relative displacement u_r greater than ± 2 mm [1]. FE analysis results showed that a prescribed displacement amplitude of ± 9 mm corresponds to the above restriction. All results for u_{top} and u_r are available in section 5.

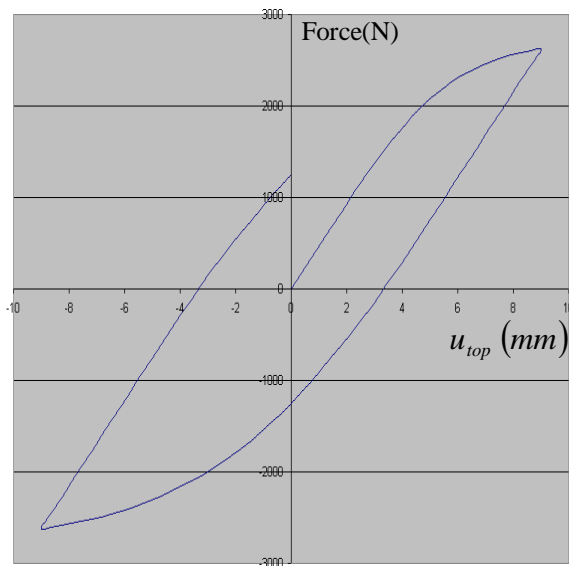
6.3.1 Effect of nail joint distribution

It is quite clear that, by increasing the number of nail joints, the damping capacity will also increase. Three different cases have been studied according to the Table 3 below.

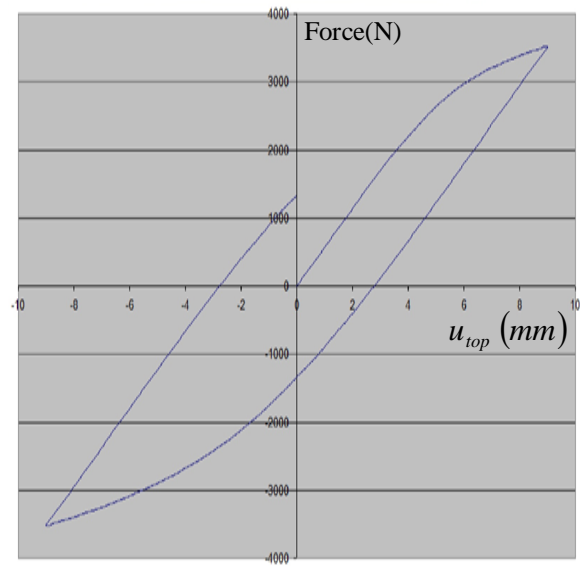
Case number	Configurations	Damping capacity [Nmm/cycle]
1	24 nail-joints, c/c 300 mm	24000
2	36 nail-joints, c/c 205 mm	26000
3	48 nail-joints, c/c 150 mm	30000

Table 3. Three different configurations for the number of nail joints.

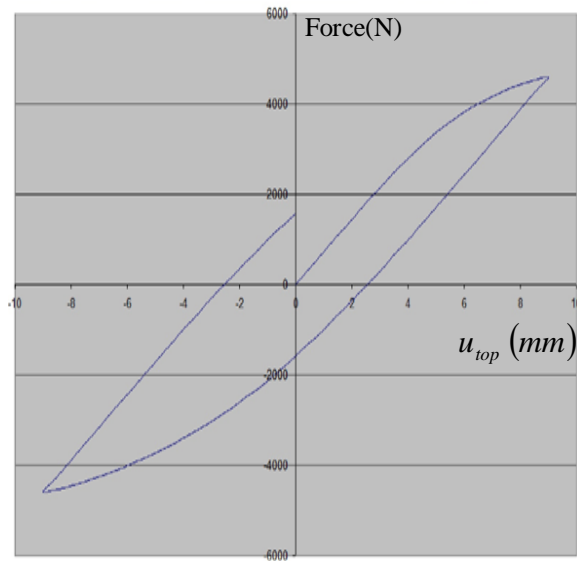
FE analysis results showed that increasing the number of nail-joints leads to increasing in the total damping capacity of the shear wall element, see Table 3 above. There is a linear relation between the number of nail joint and the total damping capacity by the shear wall element, see Figure 23.



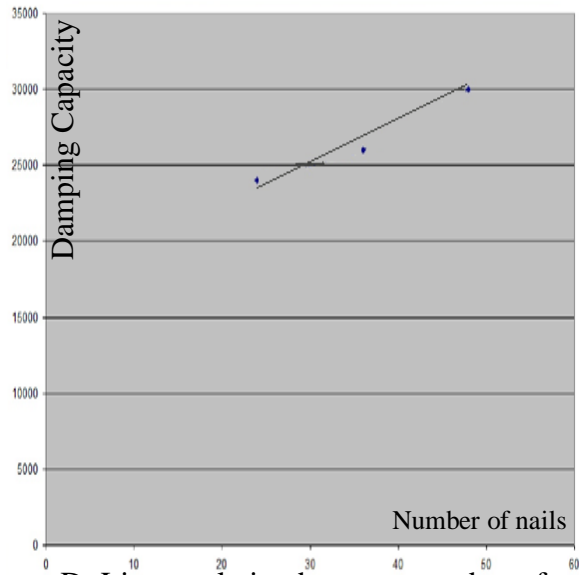
A: Damping capacity for shear wall element with 24 nail-joints.



B: Damping capacity for shear wall element with 36 nail-joints.



C: Damping capacity for shear wall element with 48 nail joint joints.



D: Linear relation between number of nail-joints and the total damping capacity.

Figure 23. A-C: Damping capacities for the standard shear wall elements with different number of nail-joints. D: Linear relation between number of nail-joints and the total damping capacity

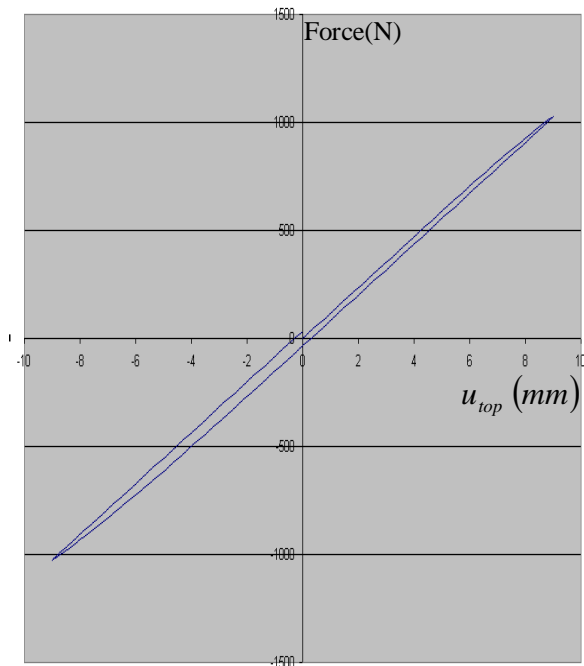
6.3.2 Influence of the panel's width

Three FE models with different width have been analyzed according to the Table 4 below. All three FE models were subjected to the prescribed top displacement amplitude of +/- 9 mm and consist of 24 nail joints.

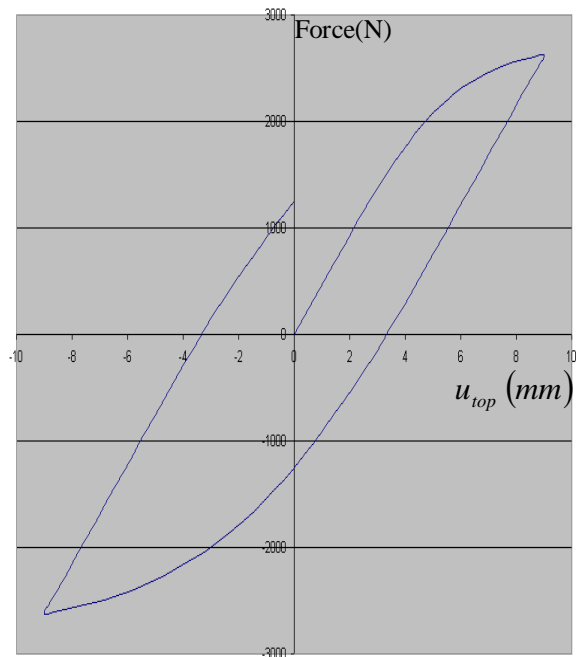
The FE analysis results show that the increasing panels' width leads to increasing the total damping capacity for the entire shear wall element. Also, the relationship between walls width and the damping capacity is almost linear; see Table 4 and Figure 24 below.

Panel's width	Damping capacity (Nmm/cycle)	Number of nail-joints
0.6 m	1000	24
1.2 m	24000	24
1.8 m	32160	24

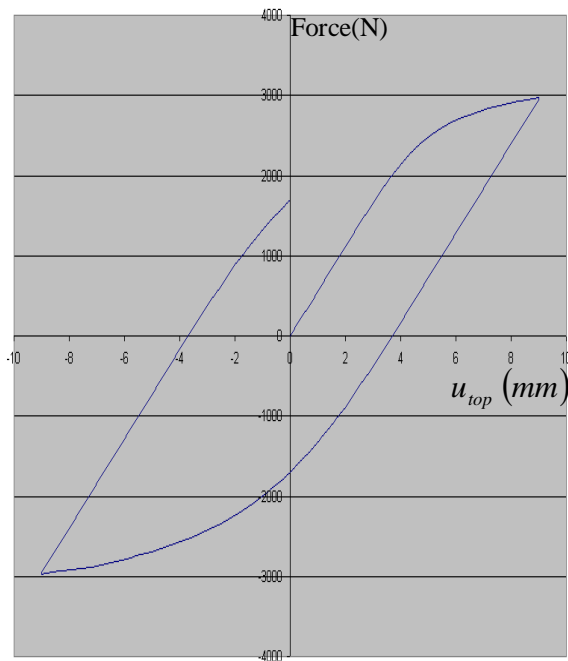
Table 4. Damping capacities for the shear wall element with different width.



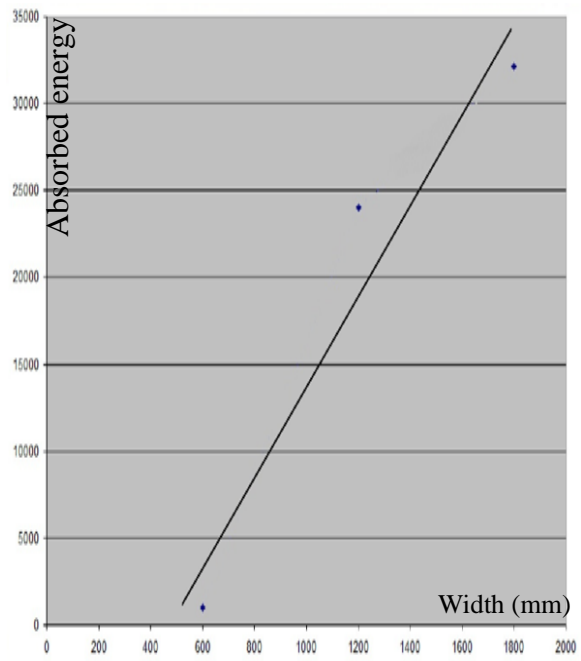
A: The damping capacity of a shear wall, width 0.6m.



B: The damping capacity of a shear wall, width 1.2m.



C: The damping capacity for a shear wall, width 1.8m.

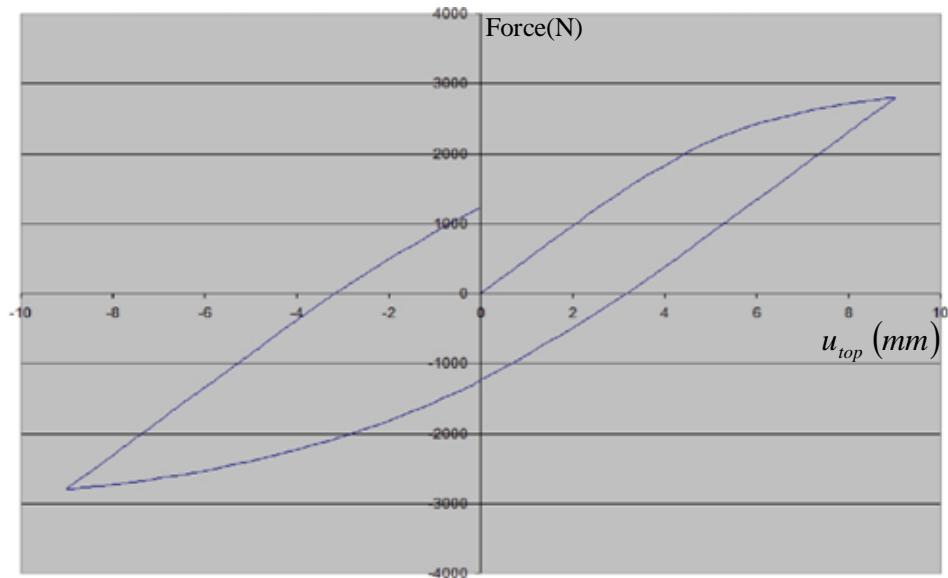


D: The relationship between the damping capacity and the width.

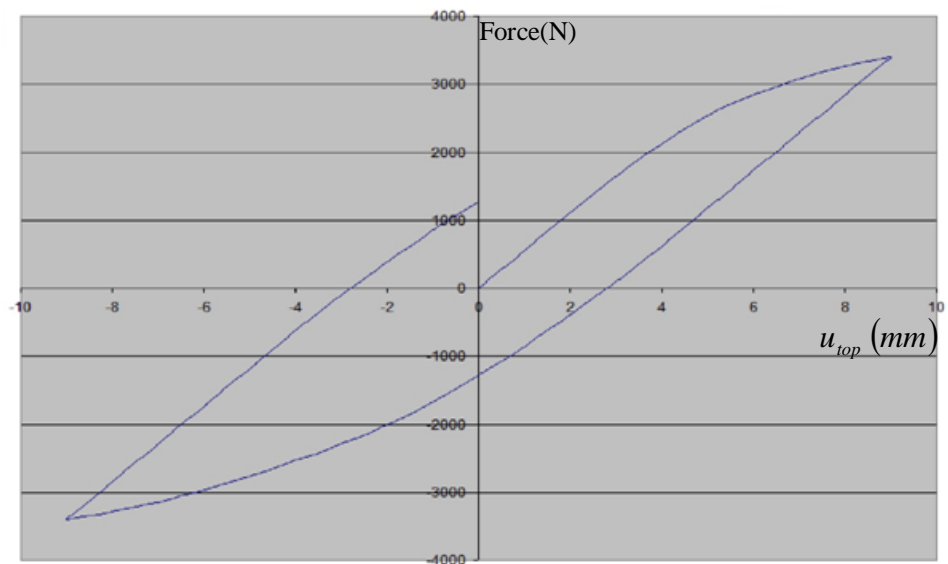
Figure 24. A-C: The relationship between the panel's width and the damping capacities of the shear wall element. D: The relationship between the damping capacity and the panel's width.

6.3.3 Influence of the middle studs

We have compared the results for two different FE models of the shear wall element. The first FE model has one middle stud at the centre of the wall and the second FE model contains two middle studs. FE analysis results showed an increasing damping capacity by using middle studs as it can be seen in Figure 25 below. Both FE models with middle studs were subjected to constant top prescribed displacement amplitude of ± 9 mm.



A: Damping capacity for the shear wall element with one middle stud ($E=26800\text{Nmm/cycle}$).



B: Damping capacity for a shear wall element with two middle studs ($E=27600\text{Nmm/cycle}$).

Figure 25. Damping capacities for the shear wall elements with A: one middle stud. B: two middle studs

6.4 Relationship between the prescribed displacement u_{top} and relative displacement $u_{rel.max}$ of the nail joint.

According to [1], see Figure 26, there is a relationship between top displacement u_{top} and relative displacement u_r

$$u_{rel.} = 0.5 * u_{top} * \sin \alpha \left[\sin^2 \alpha + \left(2 * \frac{i}{n_x} - 1 \right)^2 \cos^2 \alpha \right]^{0.5} \quad (1)$$

And the expression for the nail joint located at the top and bottom of shear wall element,

$$u_{rel.} = 0.5 * u_{top} * \sin \alpha \left[\left(2 * \frac{i}{n_y} - 1 \right)^2 \sin^2 \alpha + \cos^2 \alpha \right]^{0.5} \quad (2)$$

And the expression for the nail joints located at the left and right sides of the shear wall element

$$u_{rel.max} = 0.5 * u_{top} * \sin \alpha \quad (3)$$

Where;

α is the angle between the shear wall element diagonal and vertical stud.

n_x is the spacing between the nail units in x-direction

n_y is the spacing between the nail units in y-direction

i 0, 1, 2,, n_x

j 0, 1, 2,, n_y

$u_{rel.max}$ = Relative displacement

u_{top} = Prescribed displacement

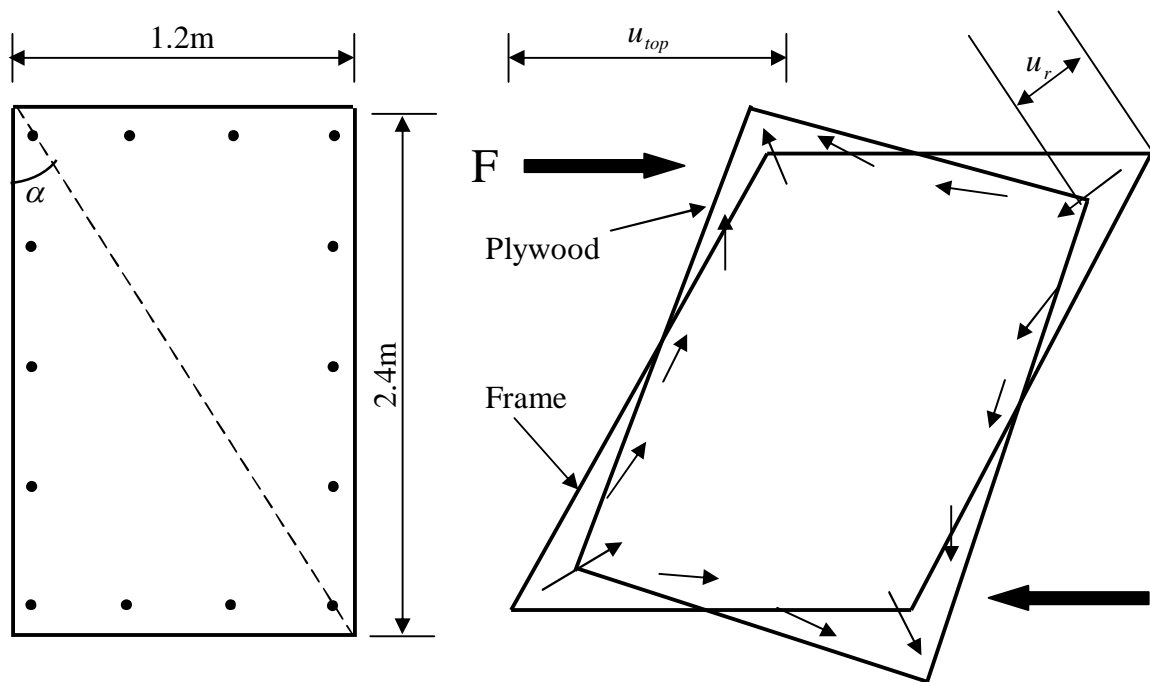


Figure 26. Shear wall element's top and relative displacements.

According to Table 2 above, case W3, we have the following data;

$$u_{r.\max} = 1.95\text{mm}$$

$$u_{top} = 9\text{mm}$$

$$\alpha = \tan^{-1} \left(\frac{1.2}{2.4} \right)$$

$$\alpha = 26,56^\circ$$

The relationship 3 gives us;

$$u_{rel.mar} = 0.5 \times 9 \times \sin 25.56 = 1.94\text{mm}$$

The difference between $u_{rel.\max}$ according to relationship (3) and the calculated $u_{rel.\max}$ of FE analysis according to the Table 2 above is only 0.5%.

7. Discussions and conclusions

In order to strengthen earthquake resistance of the wooden houses, shear walls must be designed with large damping capacity or hysteresis energy absorption. The objective must be to increase damping capacity of nail joints. And thereby limit the vibration amplitudes in the case of occurrence of an earthquake.

FE results have shown that wood-stud shear walls' damping capacity is mainly dependent on several factors such as nail-joints properties, number of nail-joints, wall dimension and the use of middle studs.

The following can be concluded from the FE analysis results:

1. Shear walls damping capacity depends mainly on the nail-joint properties.
2. Increasing the number of nail-joints leads to increasing the shear walls damping capacity.
3. If both the number of nail-joints and the height of the shear walls were kept constant then; increasing the width of the shear walls will provide higher damping capacity.
4. If the dimension of the shear wall was kept constant then; increasing the number of the middle studs will results in higher damping capacity.

8. References

8.1 literatures

- [1]. Hamid Movaffaghi and Bijan Adl-Zarrabi. Skjuvväggsselement av trä, olinjär datoranalys och förbandsprovning. Degree work, Chalmers University of Technology, Department of Civil Engineering, Division of Steel and Timber Structures, Sweden, 1991.
- [2]. ATC/SEAOC Joint Venture Training Curriculum. Seismic response of wood-frame construction, part C: the role of wood framed shear walls. Applied Technology Council (ATC) and the Structural Engineers Association of California (CEAOC).
- [3]. Timothy P. McCormick, P.E. Shear walls. Seismic Retrofit Training for Building Contractors Inspectors Publisher: Timothy P. McCormick, Edition 2005.
- [4]. Roger L.Tuomi (1978) Journal of the structural division racking strength of light frame nailed walls. Part of copyrighted Journal of the Structural Division, American Society of Civil Engineers, Vol. 104, Nr. St.7 July 1978
- [5]. Erik L. Nilson, Dan L.White.Structural Behavior of Wood Shear wall Assemblies. Experiment results of Texas University.
- [6]. Jack Porteos and Abdy Kermani. Structural Timber Design. (2007)
- [7]. Abaqus/Cae 6.8.2
- [8]. Pardoen, G.C.1, Kazanjy, R.P.2, Freund, E.3, Hamilton, C.H., Larsen, D.3, Shah, N.3, Smith A.3. Results from the city of Los Angeles-UC Irvine shear wall test program.
- [9]. Steven E. Pryor¹, Grahm W. Taylor² and Carlos E. Ventura³. Seismic Testing and Analysis Program on High Aspect Ratio Wood Shear Walls.
- [10]. Minoru OKABE¹, Naohito KAWAI², Seiji TAKADA³. Experimental analyses for estimating strength and stiffness of shear walls in wood-framed construction
- [11]. Erol Karacabeyli and Marjan Popovski. Design for Earthquake Resistance in timber engineering edited by Thelancsson S. and Larsen HJ. Wiley. Chichester Page 267-299.
- [12]. Hamid Movaffaghi. Structural Earthquake Response analysis. Doctoral Thesis, Chalmers University of Technology, Department of Applied Mechanics, Sweden, 2007.

8.2 Web resources

[13]. www.almuhandes.com

[14]. www.adrc.asia/.../image030.jpg

[15]. http://en.wikipedia.org/wiki/Shear_wall.

[16]. <http://www.abag.ca.gov/bayarea/eqmaps/fixit/manual/PT08-Ch-3B.PDF>.

[17]. www.nrc-cnrc.gc.ca/eng/ibp/irc/ctus/ctus-n45.html.

[18]. <http://earthquake.usgs.gov/earthquakes/eqarchives/year/eqstats.php>.

9. Appendix Appendix A

A1. Test specimen's dimensions

I. Selected material measurements for test specimens

- 1) Plywood: P30, $t_1 = 12mm$
- 2) OSB (Oriented Strand Board): P30, $t_1 = 12mm$
- 3) Wooden studs : T30, $t_1 \times t_2 = 50 \times 50mm^2$
- 4) Wire nail: $35 \times 17(d = 1.7mm)$
- 5) Wire nail: $35 \times 20(d = 2mm)$

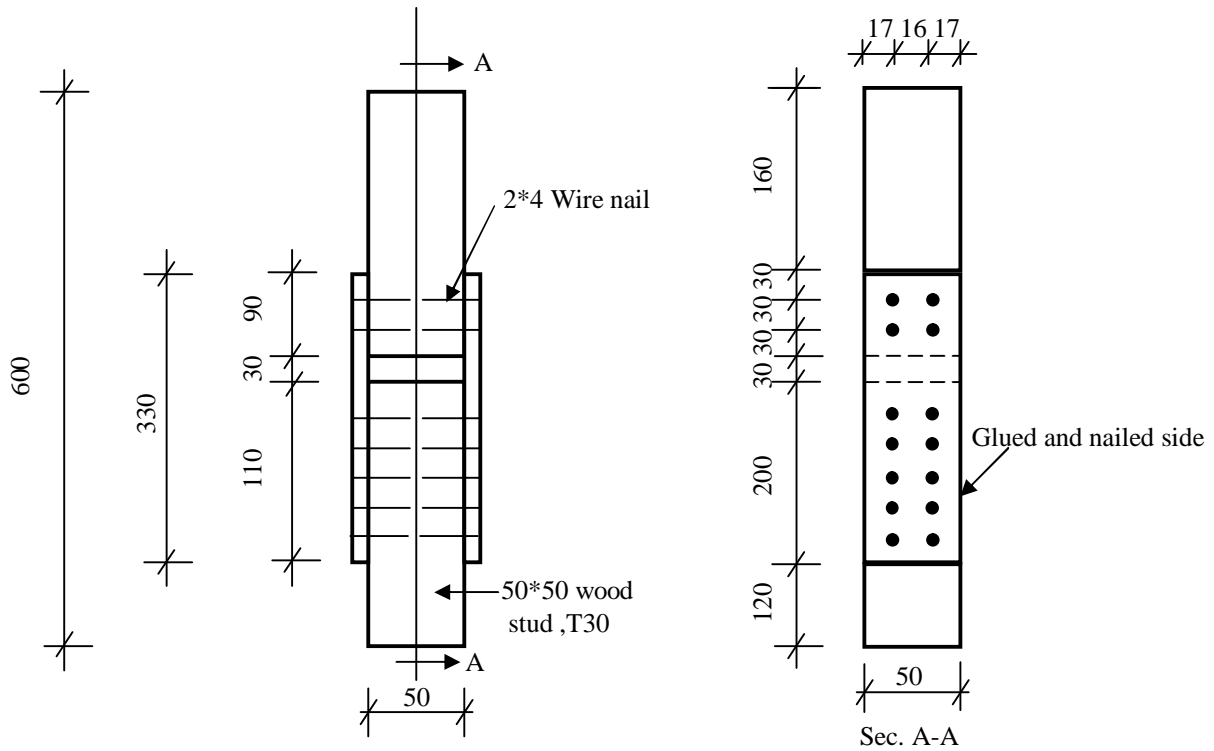


Figure A1.1. Test specimen's section and dimension

II. Material parameters for test specimens

Wooden stud: T30, $E = 6000MPa$

Plywood: P30, $t = 12mm, I = 360mm, E = 10000MPa$

Wire nail: $35 \times 17, \sigma_s = 600MPa$

Wire nail: $35 \times 20, \sigma_s = 600MPa$

A2. Nail-joints' force-displacement relation

The purpose of the experiments was to determine the damping capacity of the nail-joint which would represent a beam element with the same damping capacity in the FE model.

The shaded area in Figure A2.1 shows half of the total damping capacity per cycle, therefore, $E = 2000 \times 2 = 4000 \text{ Nmm/cycle}$ is the total damping capacity for 8 nails (i.e. 4 joints).

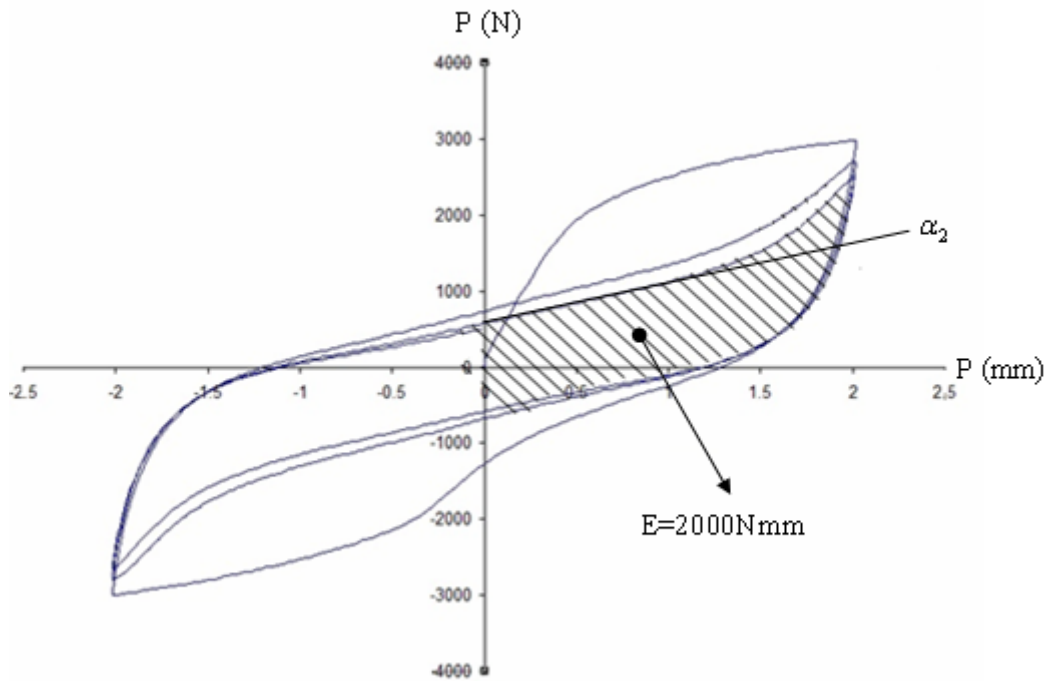


Figure A2.1. The shaded part shows half of the total damping capacity per cycle of the nail joint with 8 nails.

Thus damping capacity for 2 nails (one from each side) will be $E = 1000 \text{ Nmm/cycle}$. The hatched area A_1 in Figure A2.2 restricted by (second and third loops slope in Figure A2.1) and + 2 mm displacement line, representing half of the total damping capacity per cycle of the nail-joint with 2 nails.

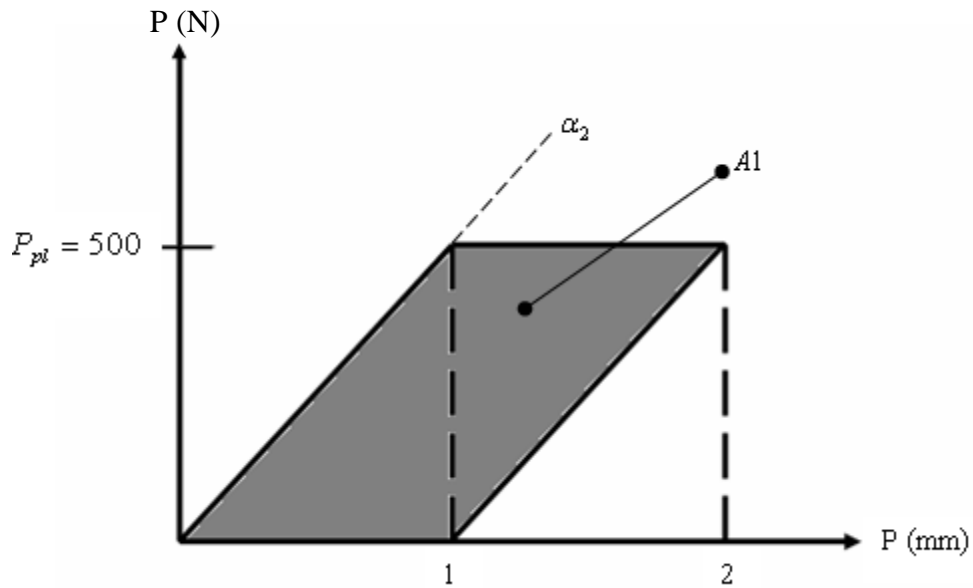


Figure A2.2. The shaded area shows half of the total damping capacity per cycle of the nail joint.

Then, we could evaluate the equivalent Young modulus and yield stress for corresponding beam elements as described in A3.

A3. Conversion of nail joint's force-displacement curve to stress-strain relation

The purpose of the laboratory experiments was to determine the stress-strain relationship for a nail joint. The material model has later been used for the beam elements that represent the nail joint in the FE model of a shear wall element, see section 4.3.

We have approximated the nail-joint in Figure A3.1 to a beam element with boundary conditions as in Figure A3.2.

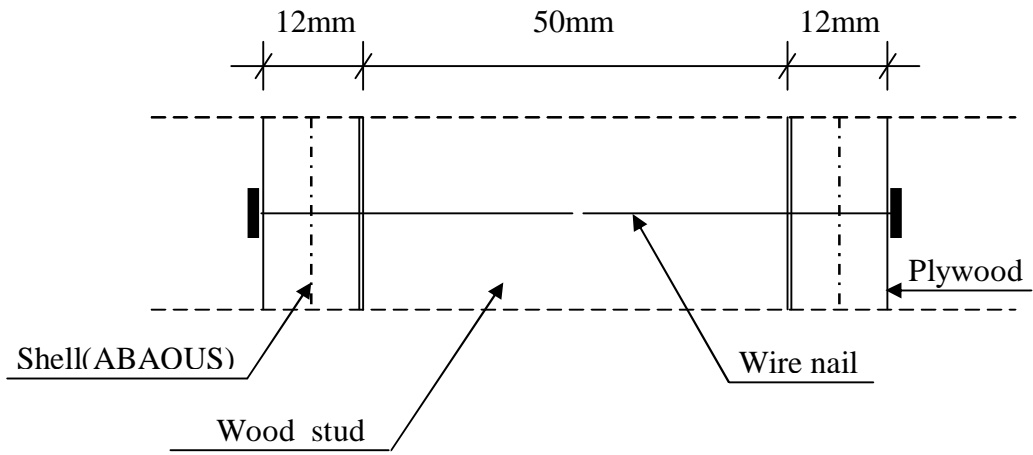


Figure A3.1. Nail joint's components

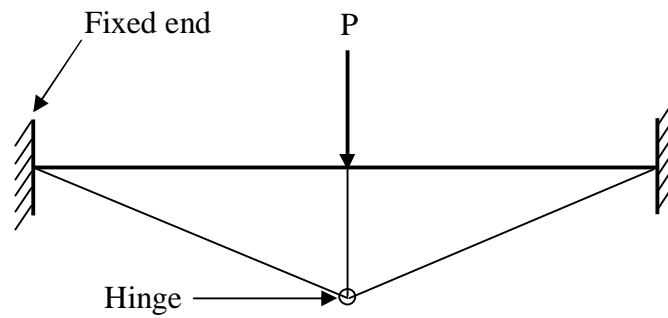


Figure A3.2. The approximate beam element for nail-joint with associated plastic deformation.

For a beam element as in figure A3.2, the following is applied;

$$\sigma_s = \frac{M_{pl}}{Z} \quad (1)$$

$$\delta_{pl} = \frac{PL^3}{3EI} \quad (2)$$

Where:

$$M_{pl} = P_{pl} \times L = 250 \times 31 = 7750 Nmm \text{ (By symmetry)}$$

$$I = \frac{bh^3}{12} = \frac{(1.5 \times 10^{-3})^4}{12} = 0.422 mm^4$$

$$Z = \frac{bh^2}{4} = \frac{(1.5 \times 10^{-3})^3}{4} = 0.844 \text{ mm}^3$$

$$L = 62 \text{ mm}$$

$$\delta_{pl} = 1 \text{ mm}$$

$$(1) \Rightarrow \sigma_s = \frac{7750}{0.844} = 9.182 \times 10^3 \text{ N/mm}^2$$

$$(2) \Rightarrow E = \frac{PL^3}{3 \times \delta_{pl} \times I} = \frac{250 \times 31^3}{3 \times 1 \times 0.422} = 5.88 \times 10^6 \text{ N/mm}^2$$

Conclusions:

$$\sigma_s = 9.182 \times 10^3 \text{ N/mm}^2$$

$$E = 5.88 \times 10^6 \text{ N/mm}^2$$

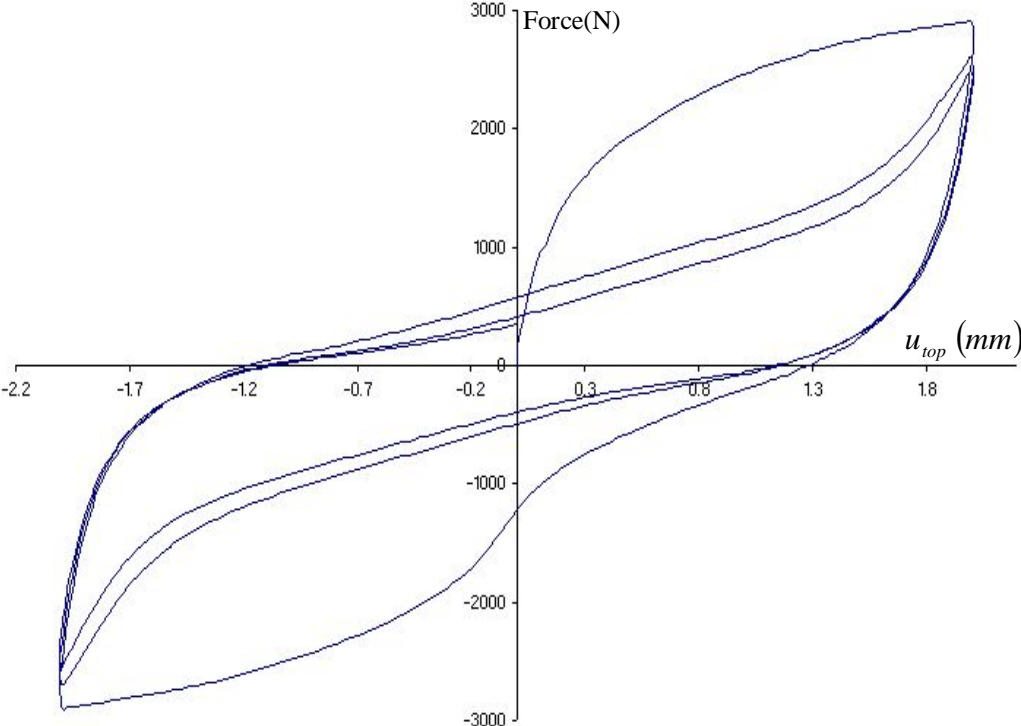
$$b' = h' = 1.5 \times 10^{-3} \text{ m}$$

Appendix B

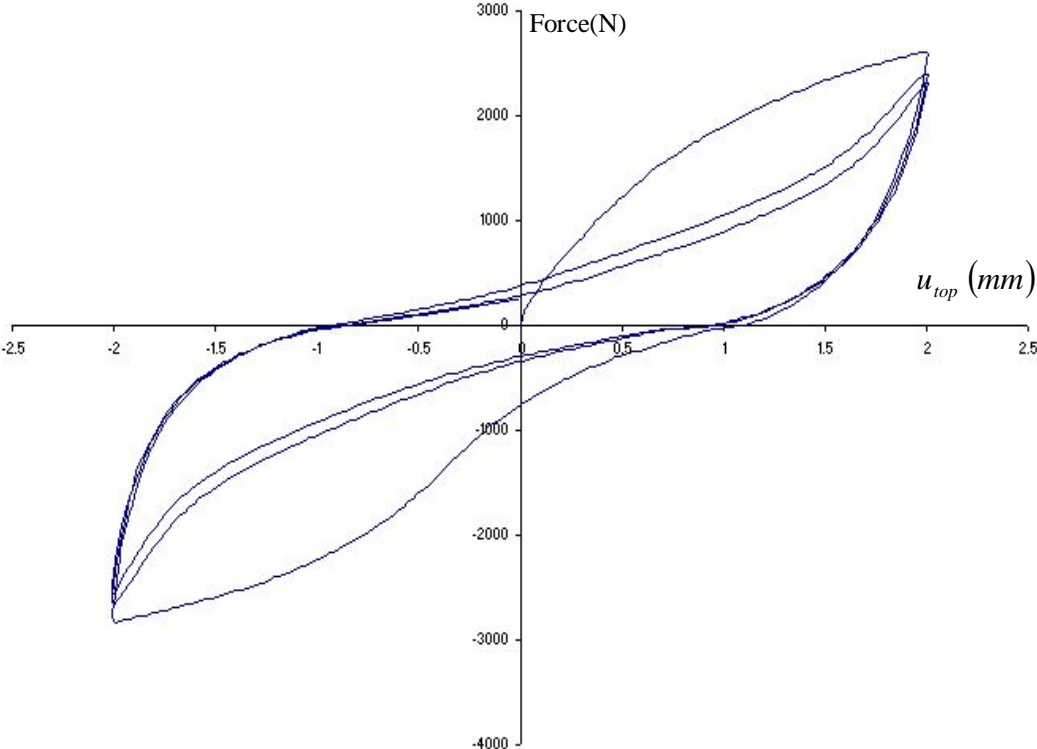
Test Specimens' force-displacement curves from experiments. Totally 16 specimens were loaded. Figures below are showing all 16 curves.

1. Specimens A-01 to A-04

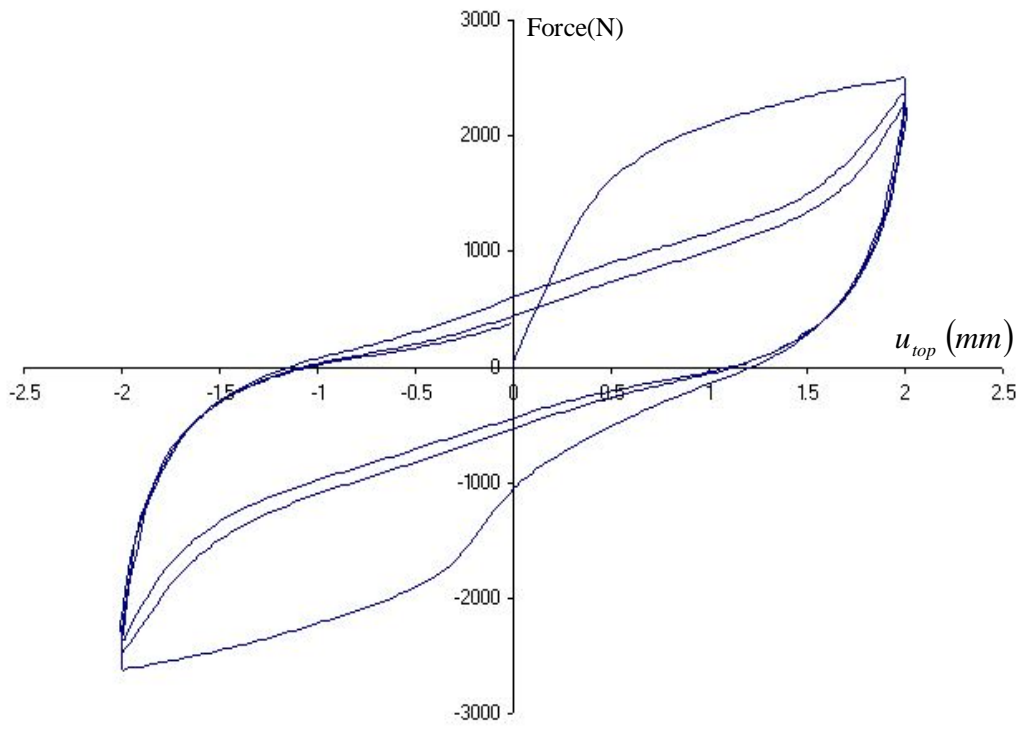
A-01



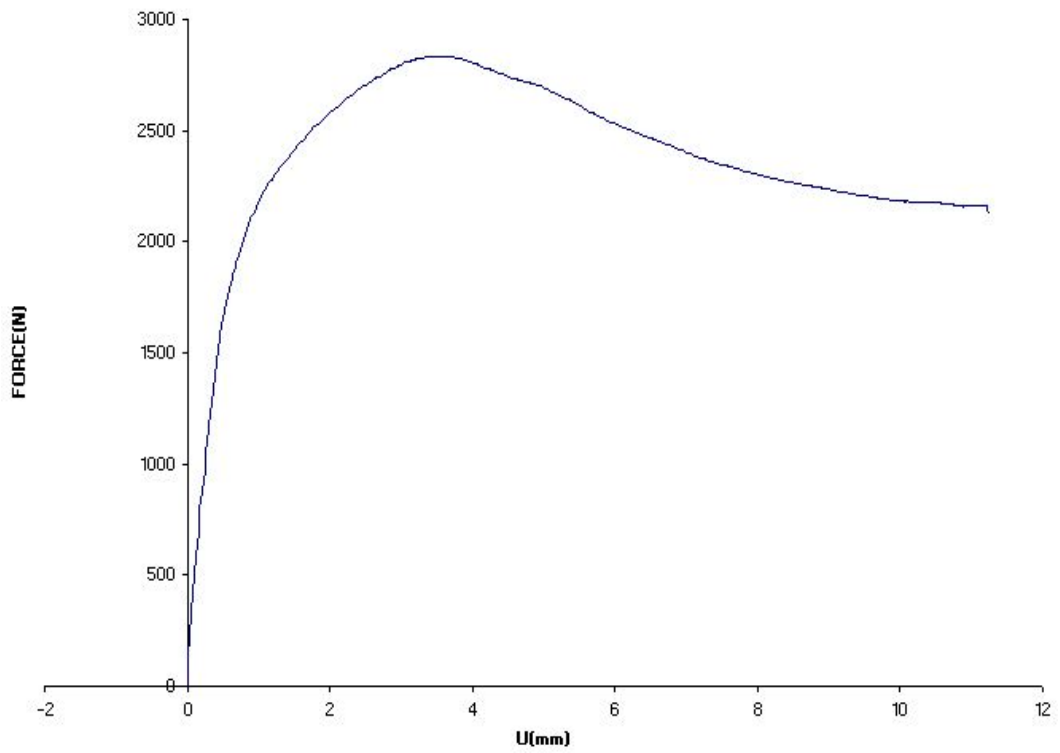
A-02



A-03

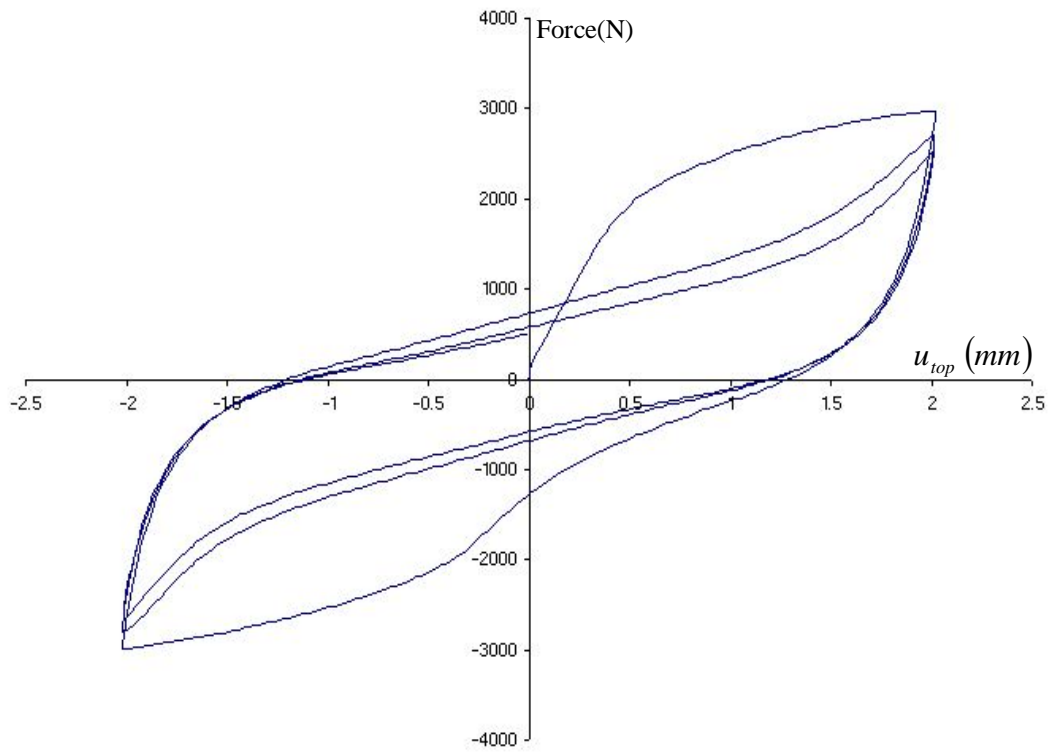


Failure load A-04

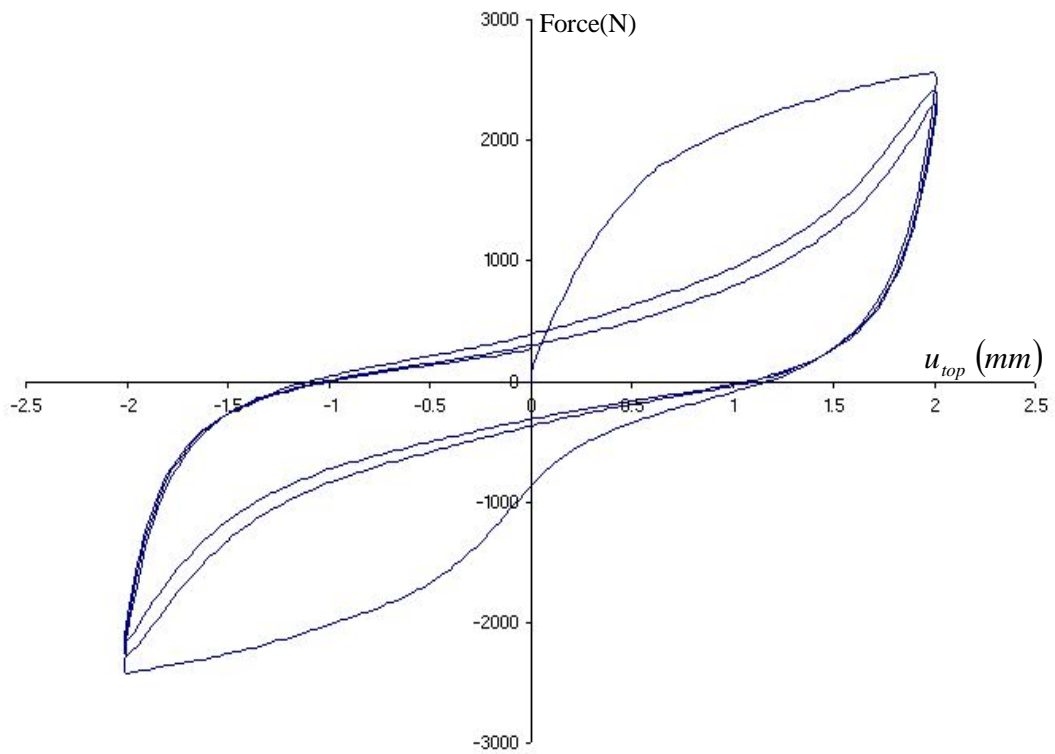


2. Specimens B-01 to B-04

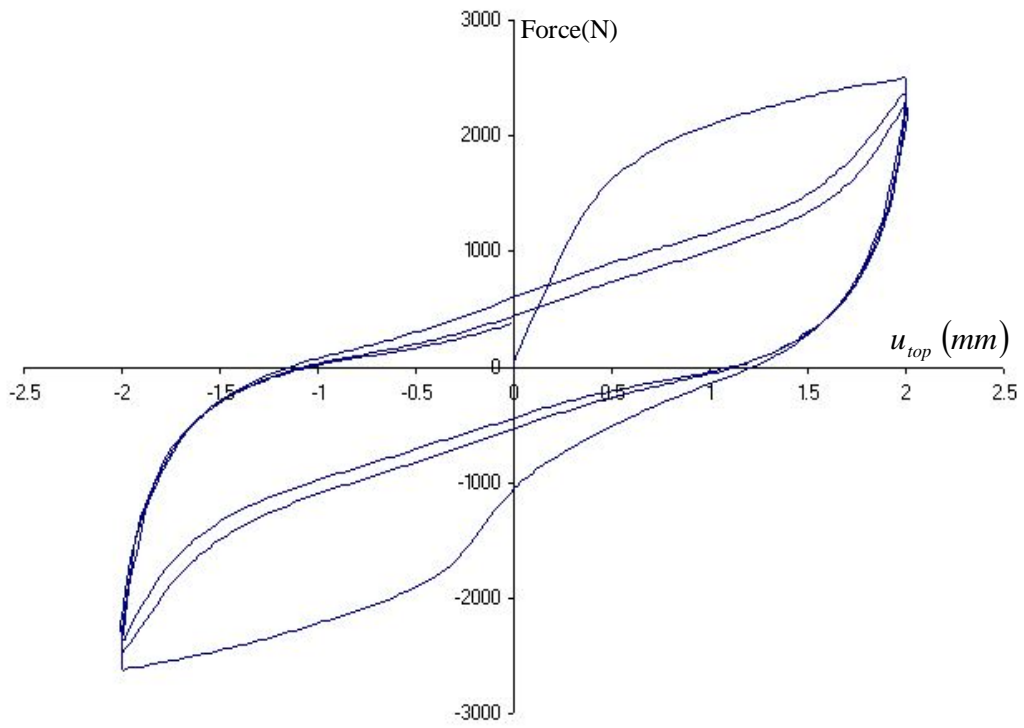
B-01



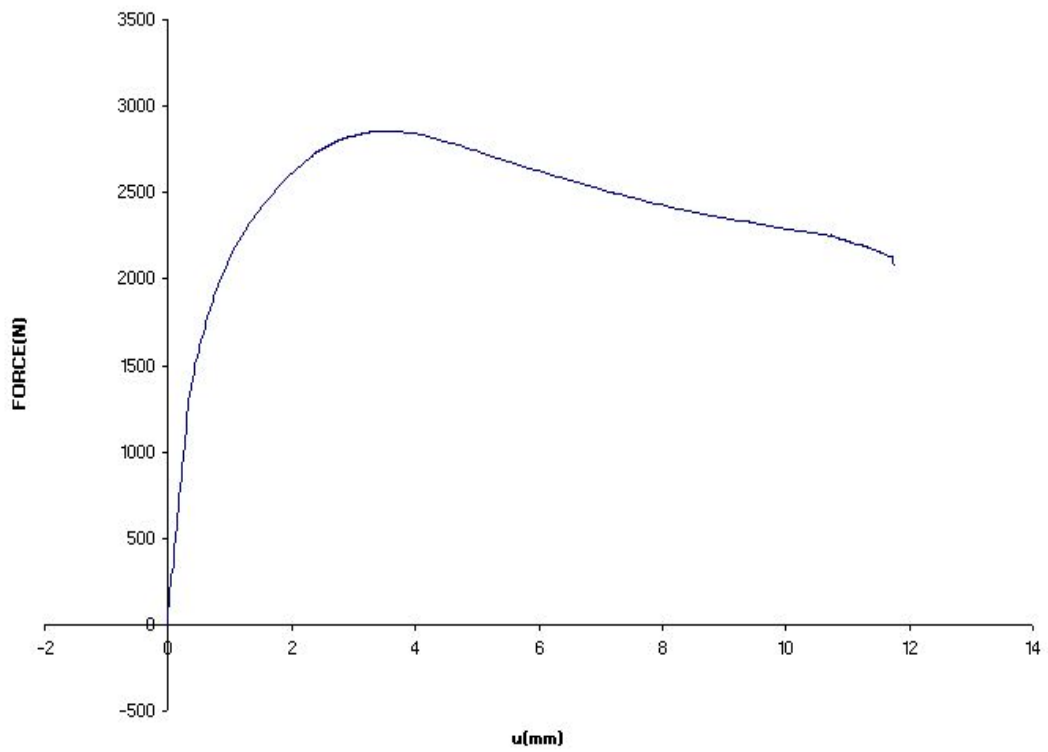
B-02



B-03

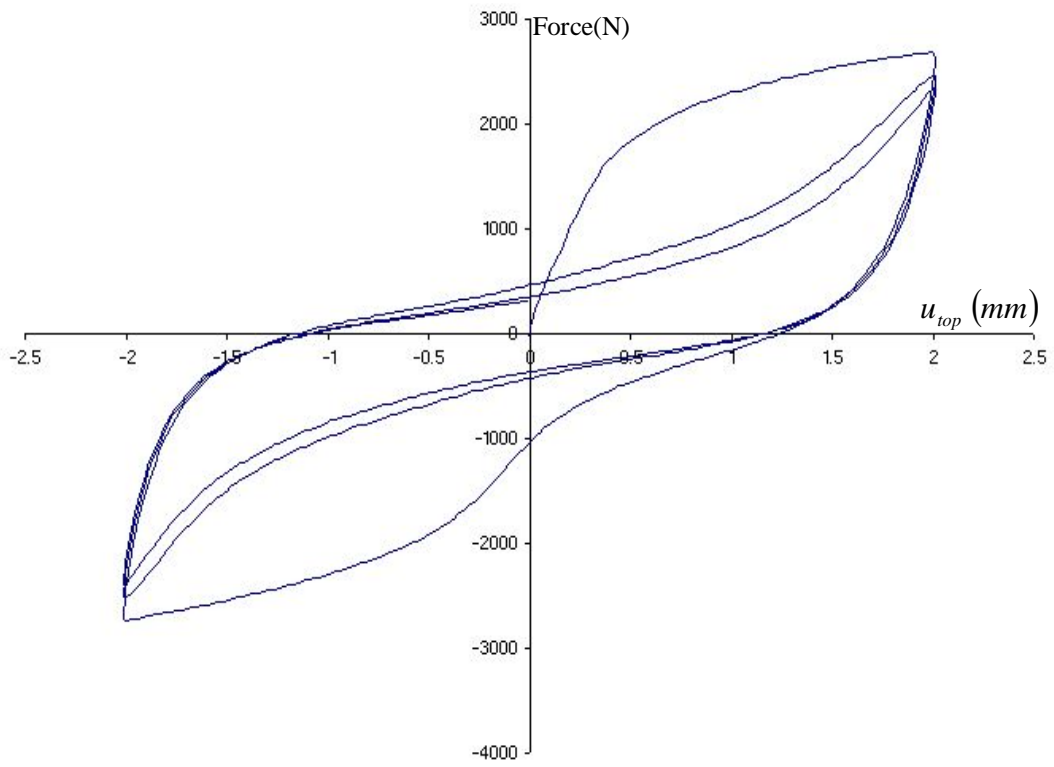


Failure load B-04

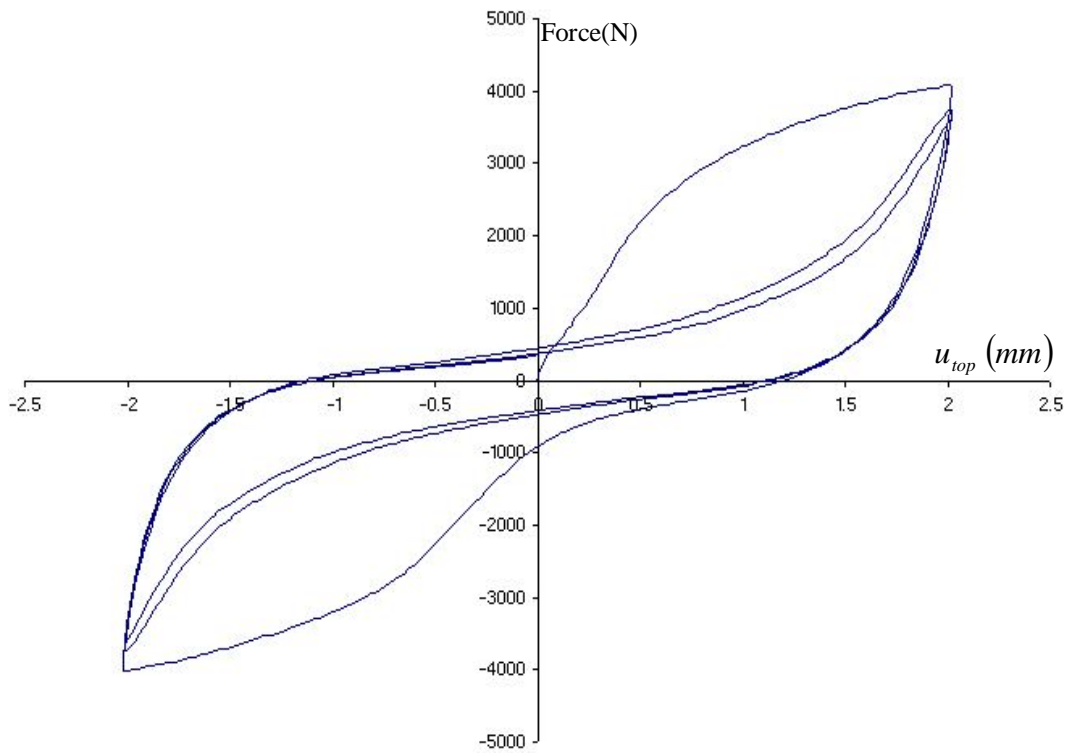


3. Specimens C-01 to C-04

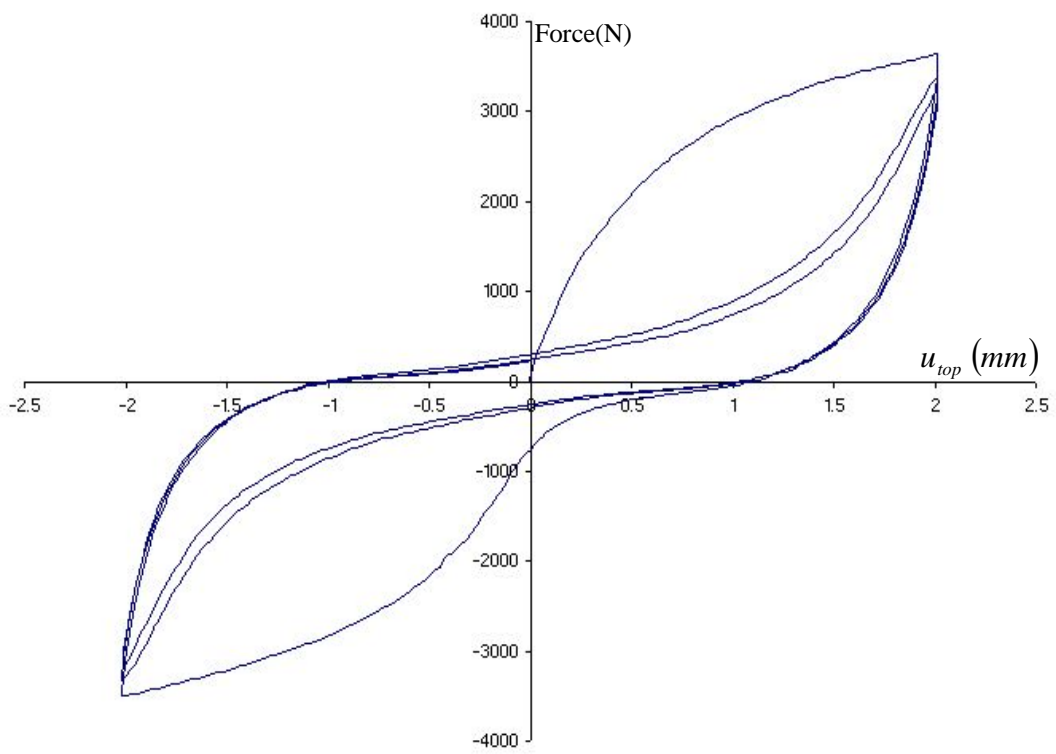
C-01



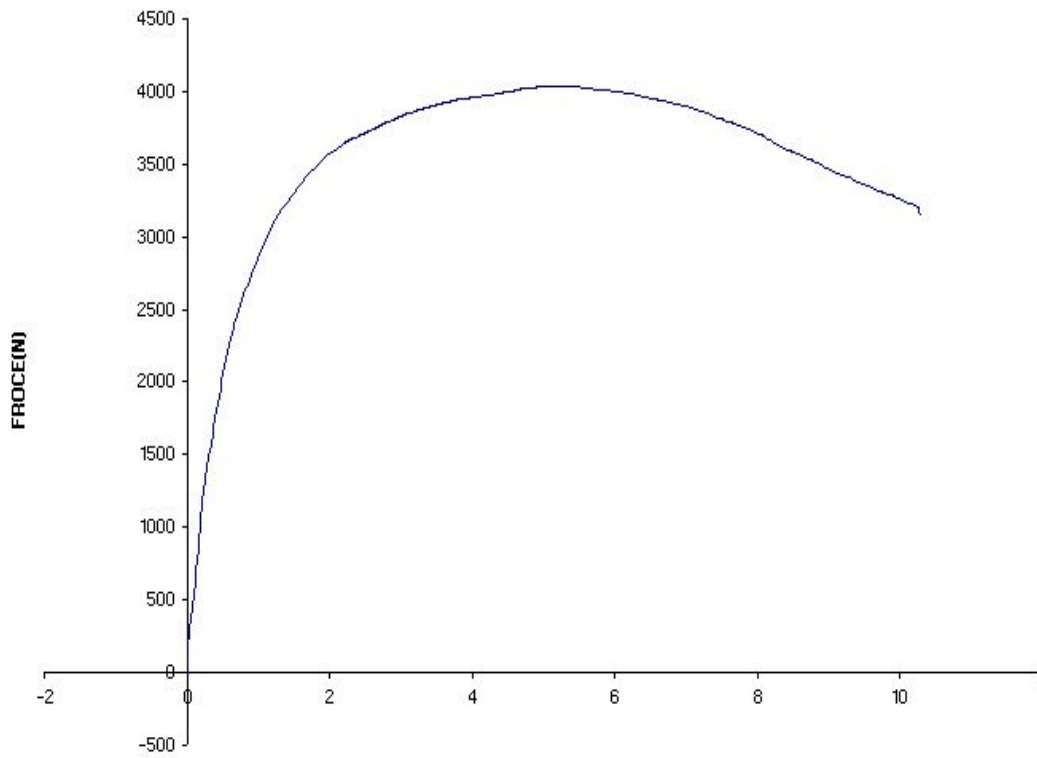
C-02



C-03

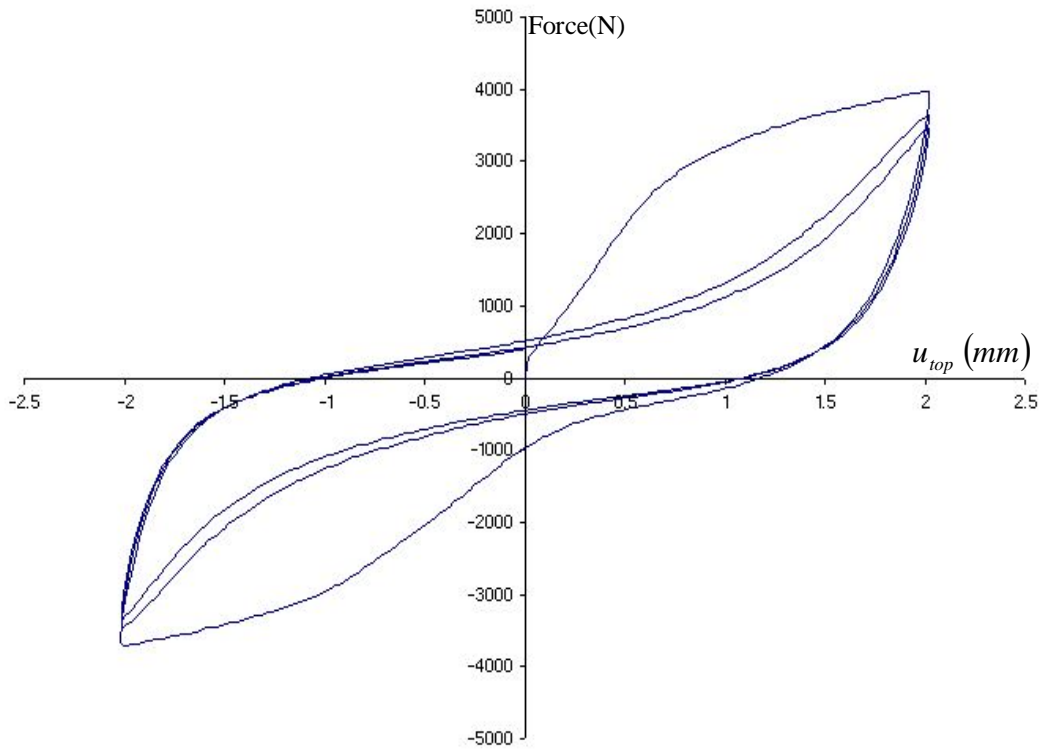


Failure load C-04

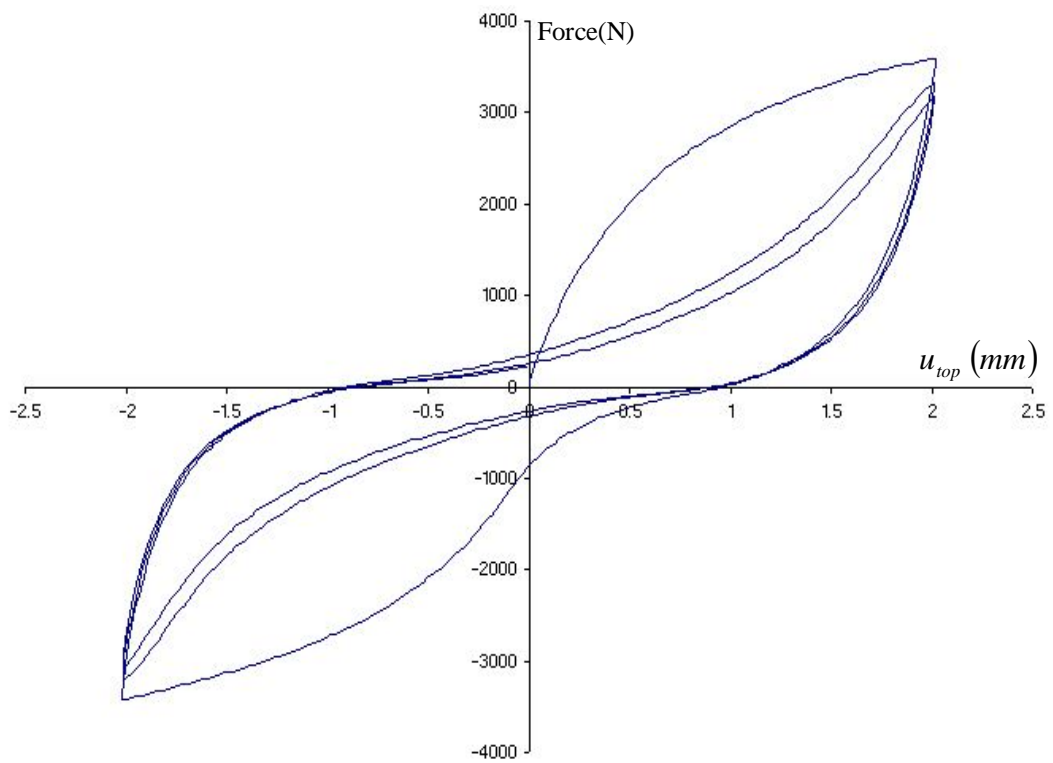


4. Specimens D-01 to D-04

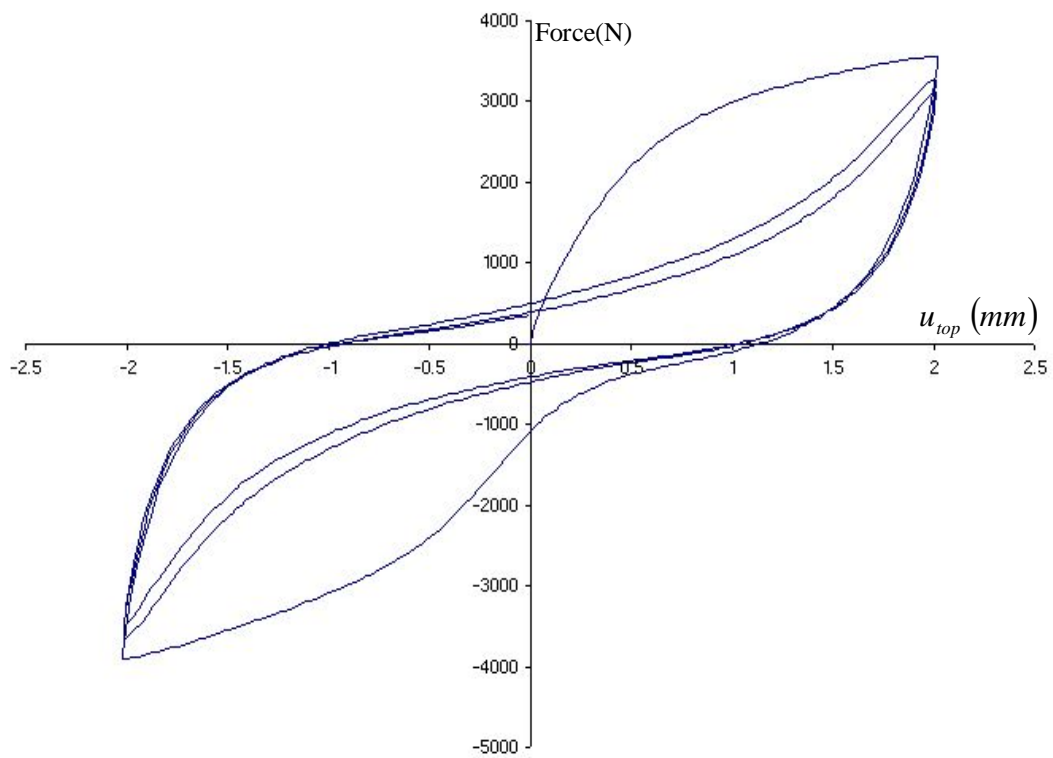
D-01



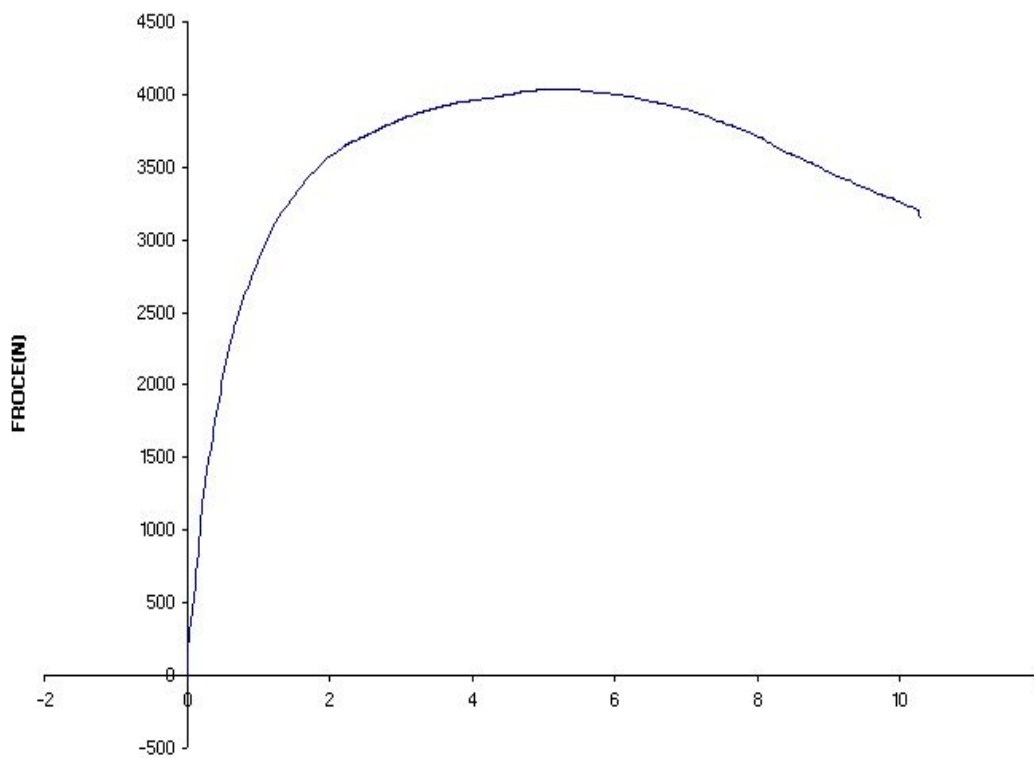
D-02



D-03



Failure load D-04



Appendix C

The following Figures shows the damping capacity for different FE model of the shear wall element

C1. Model W1

Dimension $(0.6*2.4)m^2$, number of nails 24, $u_{top} = \pm 9mm$

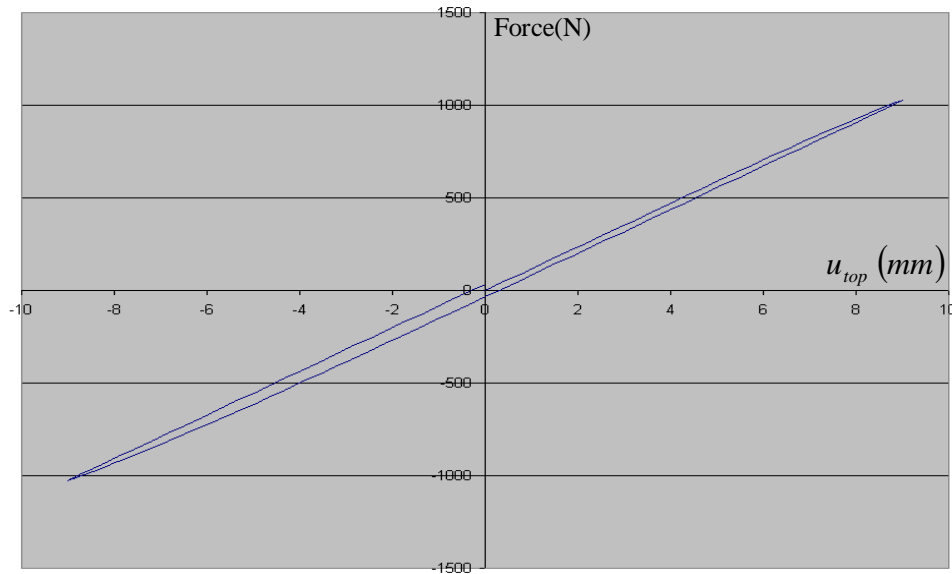


Figure C1.1. Damping capacity for the shear wall element.

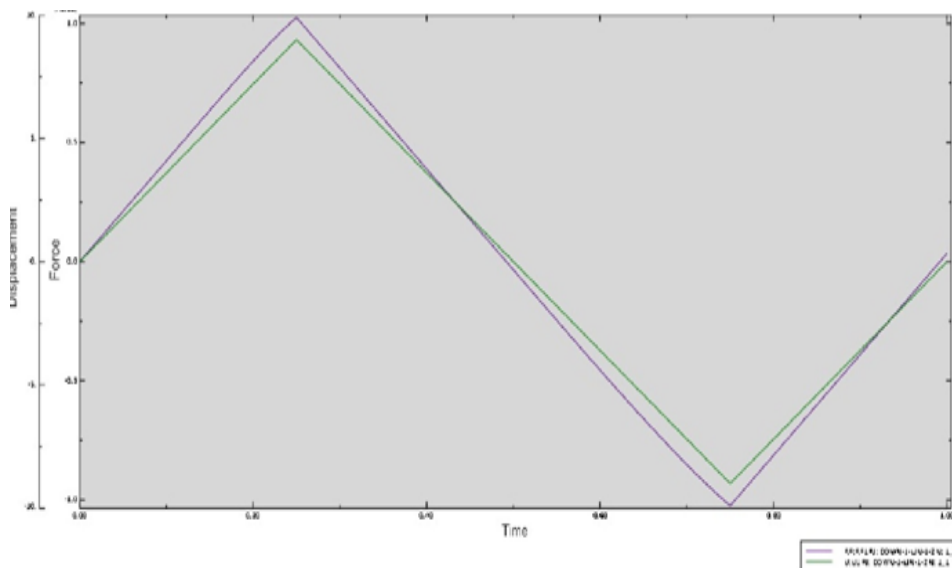


Figure C1.2. Force and displacement versus time during the cyclic loading.

C2. Model W2

Dimension $(1.8 \times 2.4) m^2$, number of nails 24, $u_{top} = \pm 9 mm$

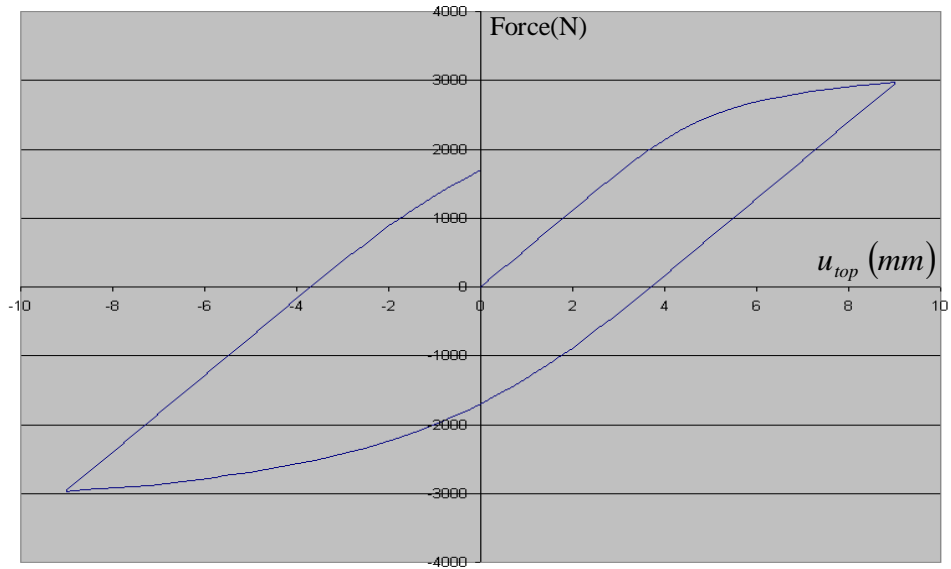


Figure C2.1. Damping capacity for the shear wall element.

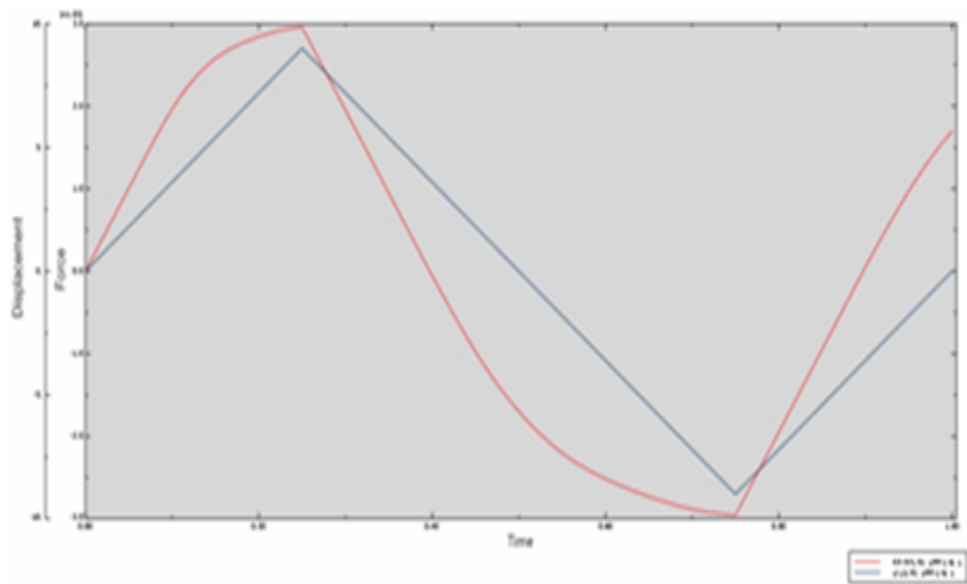


Figure C2.2. Force and displacement versus time during the cyclic loading.

C3. Model W3

Dimension $(1.2*2.4)m^2$, number of nails 24, $u_{top} = \pm 9mm$

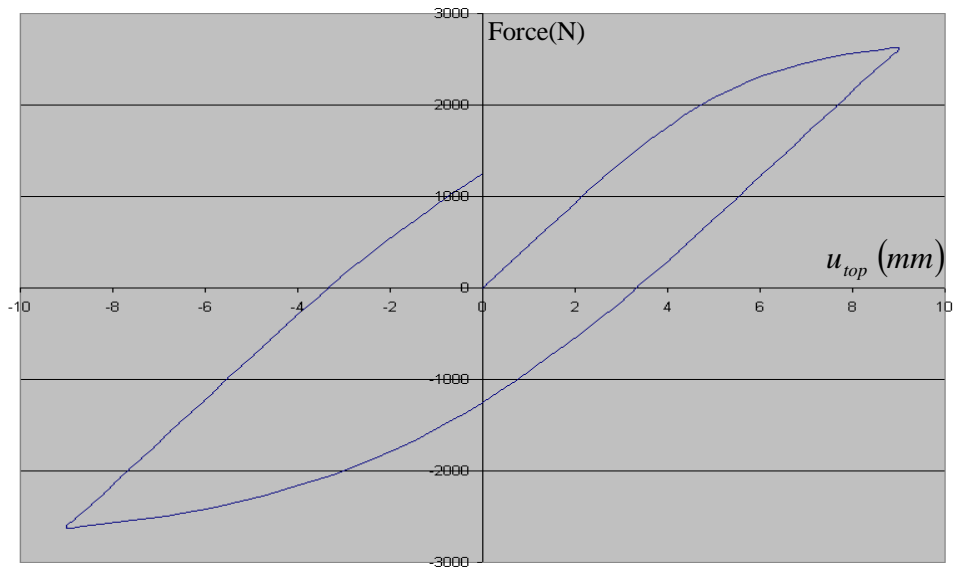


Figure C3.1. Damping capacity for the shear wall element.

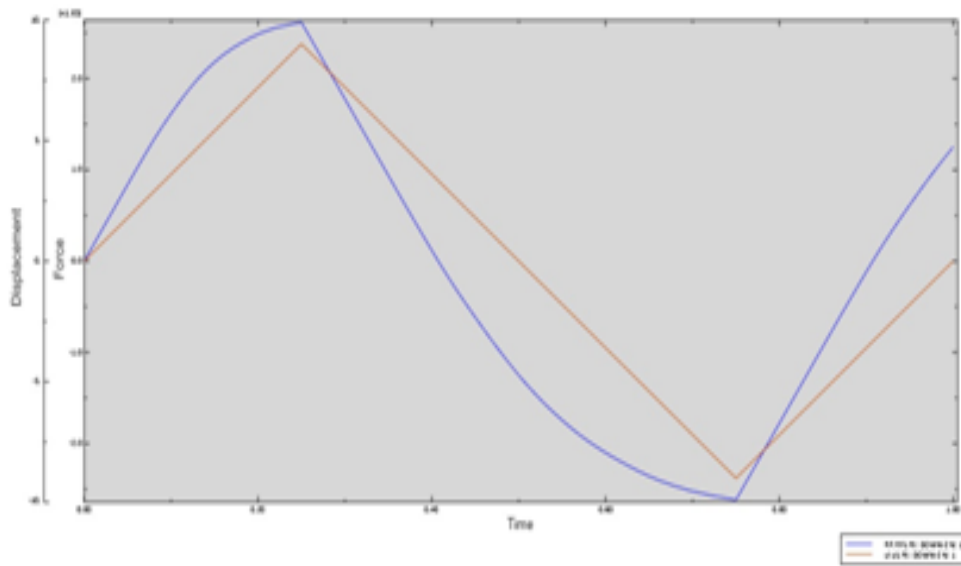


Figure C3.2. Force and displacement versus time during the cyclic loading.

C4. Model W4

Dimension $(1.2 \times 2.4) m^2$, number of nails 36, $u_{top} = \pm 9 mm$

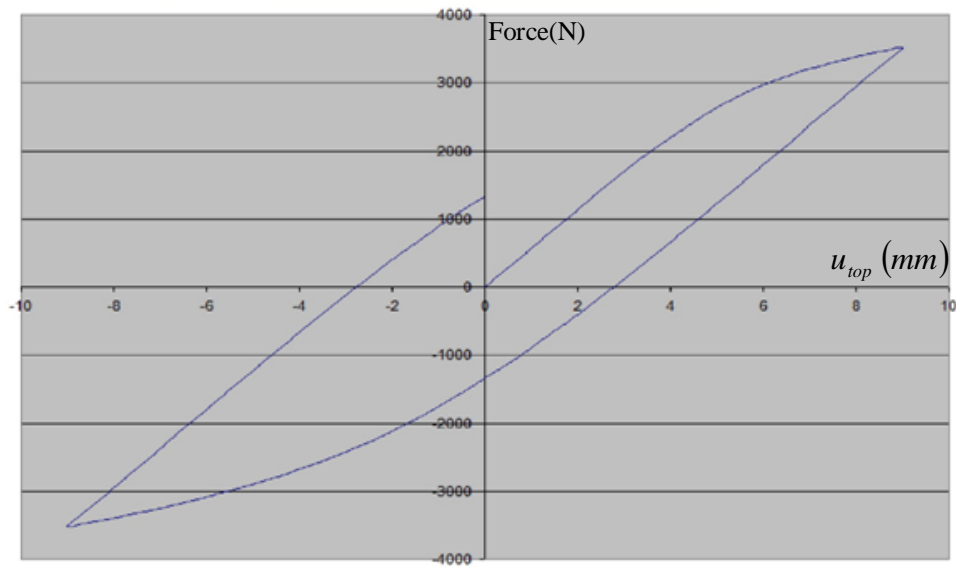


Figure C4.1. Damping capacity for the shear wall element.

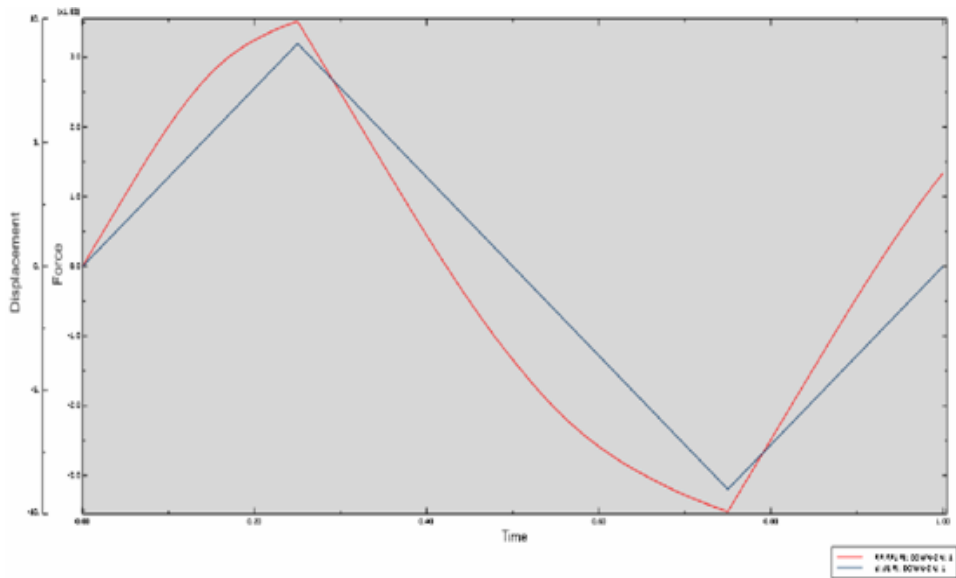


Figure C4.2. Force and displacement versus time during the cyclic loading.

C5. Model W5

Dimension $(1.2 \times 2.4) m^2$, number of nails 48, $u_{top} = \pm 9 mm$

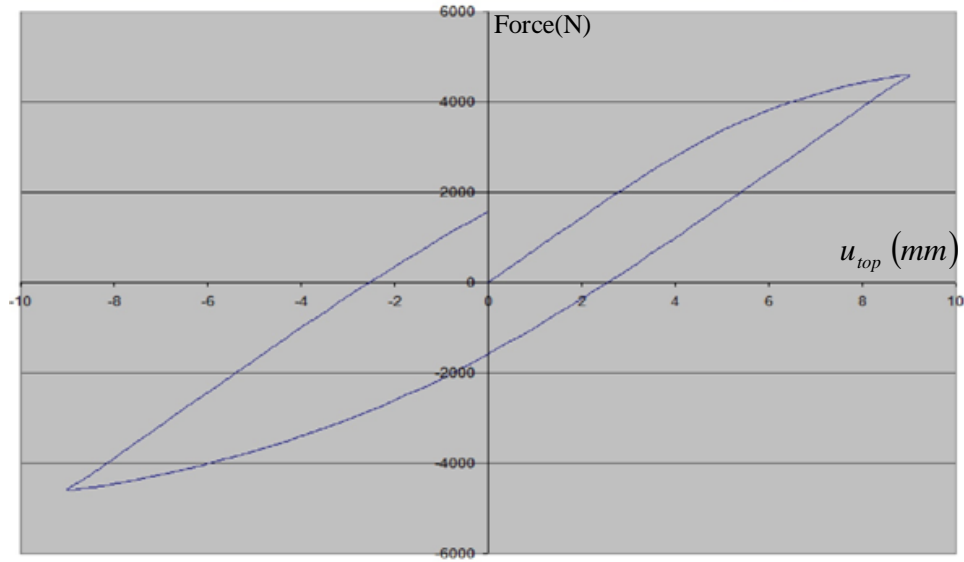


Figure C5.1. Damping capacity for the shear wall element.

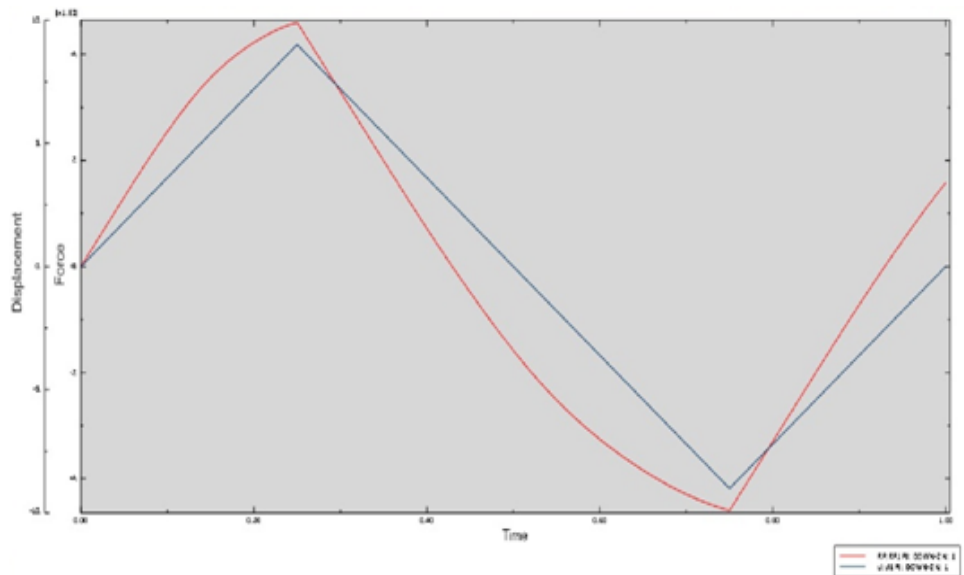


Figure C5.2. Force and displacement versus time during the cyclic loading.

C6. Model W6

Dimension $(1.2*2.4)m^2$, one middle stud, number of nails 33, $u_{top} = \pm 9mm$

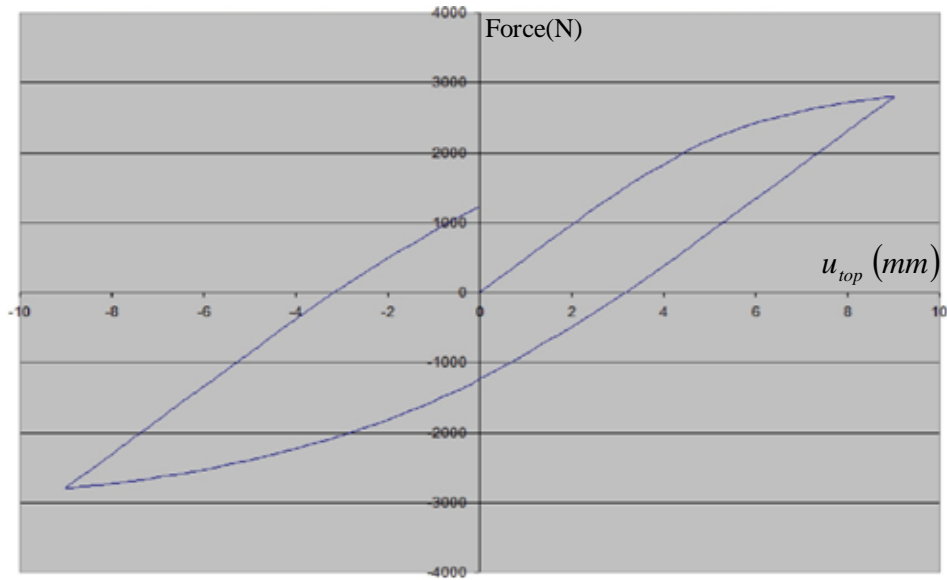


Figure C6.1. Damping capacity for the shear wall element.

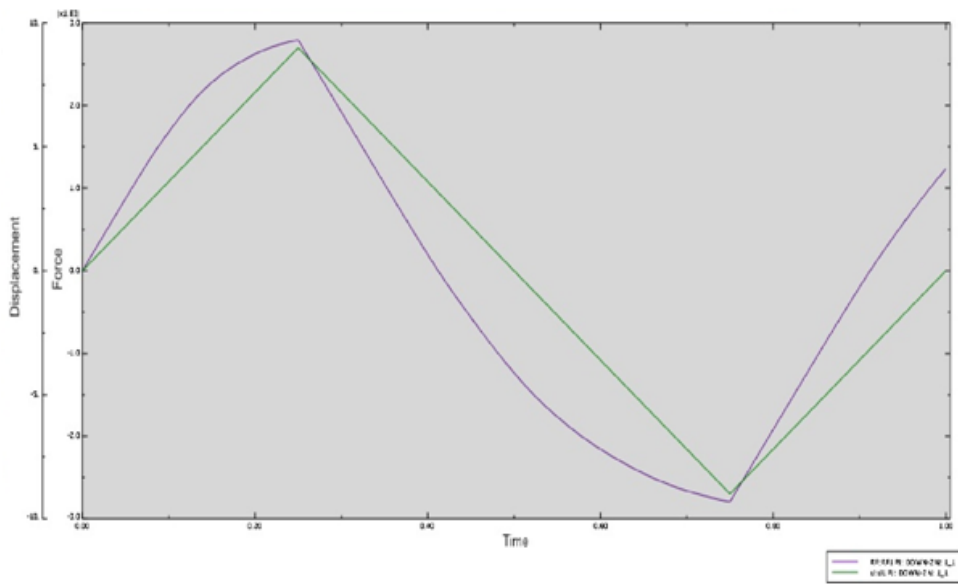


Figure C6.2. Force and displacement versus time during the cyclic loading.

C7. Model W7

Dimension $(1.2*2.4) m^2$, tow middle studs, number of nails 38, $u_{top} = \pm 9mm$

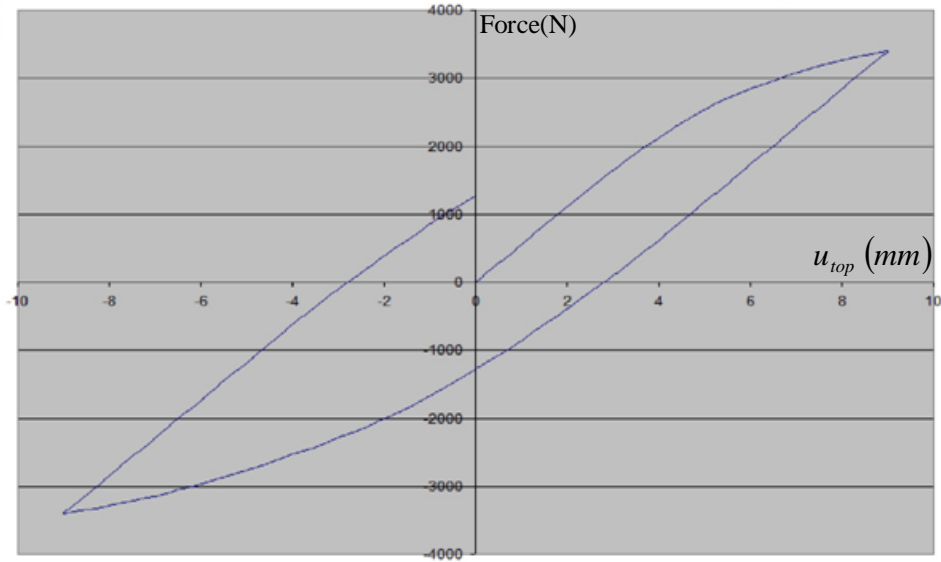


Figure C7.1. Damping capacity for the shear wall element.

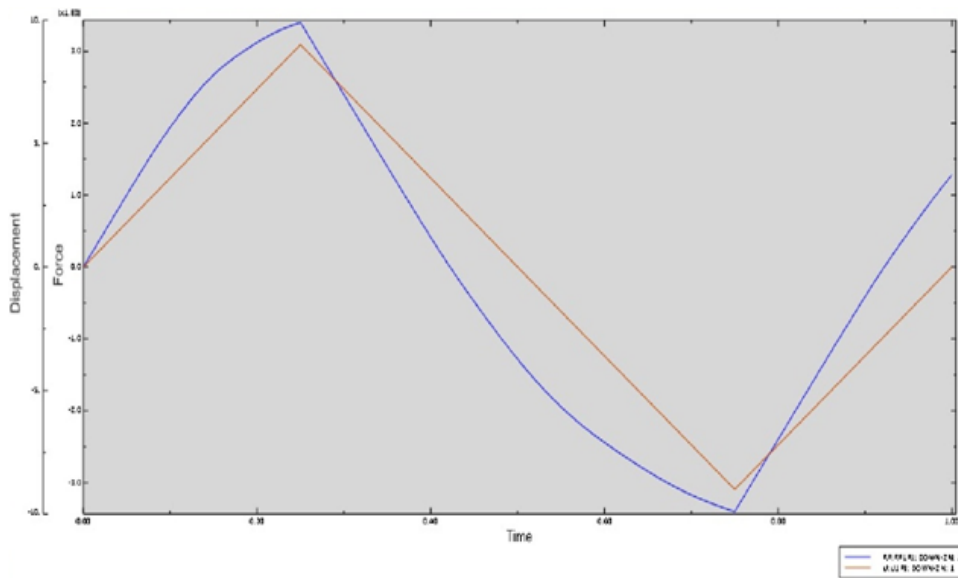


Figure C7.2. Force and displacement versus time during the cyclic loading.